Supplemental information about the prescribed chemical boundary conditions and emission inventories used for the ESCiMo simulations

This document is part of the electronic supplement to our article
"Earth System Chemistry Integrated Modelling (ESCiMo) with the Modular Earth Submodel System (MESSy, version 2.51)"
in Geosci. Model Dev. Discuss. (2015), available at:
http://www.geosci-model-dev-discuss.net

Date: September 10, 2015

Contents

1 Introduction **3**

2 Prescribed boundary conditions **3**

3 Prescribed boundary conditions for spin-up simulations with coupled ocean model **11**

4 Prescribed anthropogenic emissions **13**

4.1 Naming conventions . . . 13

4.2 Description of the inventories . . . 14

4.2.1 MACCity . . . 14

4.2.2 ACCMIP+AR5/RCP6.0 . . . 14

4.2.3 Notes on the NMHC emissions . . . 15

4.2.4 Notes on the ACCMIP emissions . . . 15

4.3 Comparison of inventories by sector . . . 16

4.3.1 Biomass burning . . . 16

4.3.2 Road traffic . . . 20

4.3.3 Agricultural waste burning . . . 24

4.3.4 Shipping . . . 28

4.3.5 Aviation . . . 31

4.3.6 Land without road and awb . . . 32

4.3.7 Anthropogenic emissions without emissions from aviation . . . 36

4.4 Remarks . . . 40

4.5 Emissions of diagnostic tracers . . . 40

5 Non-anthropogenic emissions **42**

6 Boundary conditions for on-line calculated emissions **44**

References **48**

1 Introduction

This document provides an overview of the prescribed chemical boundary conditions and emission inventories used for the ESCiMo simulations.

2 Prescribed boundary conditions

For species with uncertain emission fluxes pseudo-emissions are calculated by the submodel TNUDGE (Kerkweg et al., 2006). The simulated mixing ratios in the lowest model layer are relaxed by Newtonian relaxation to observed or projected surface mixing ratios (Figures E1 – E7).

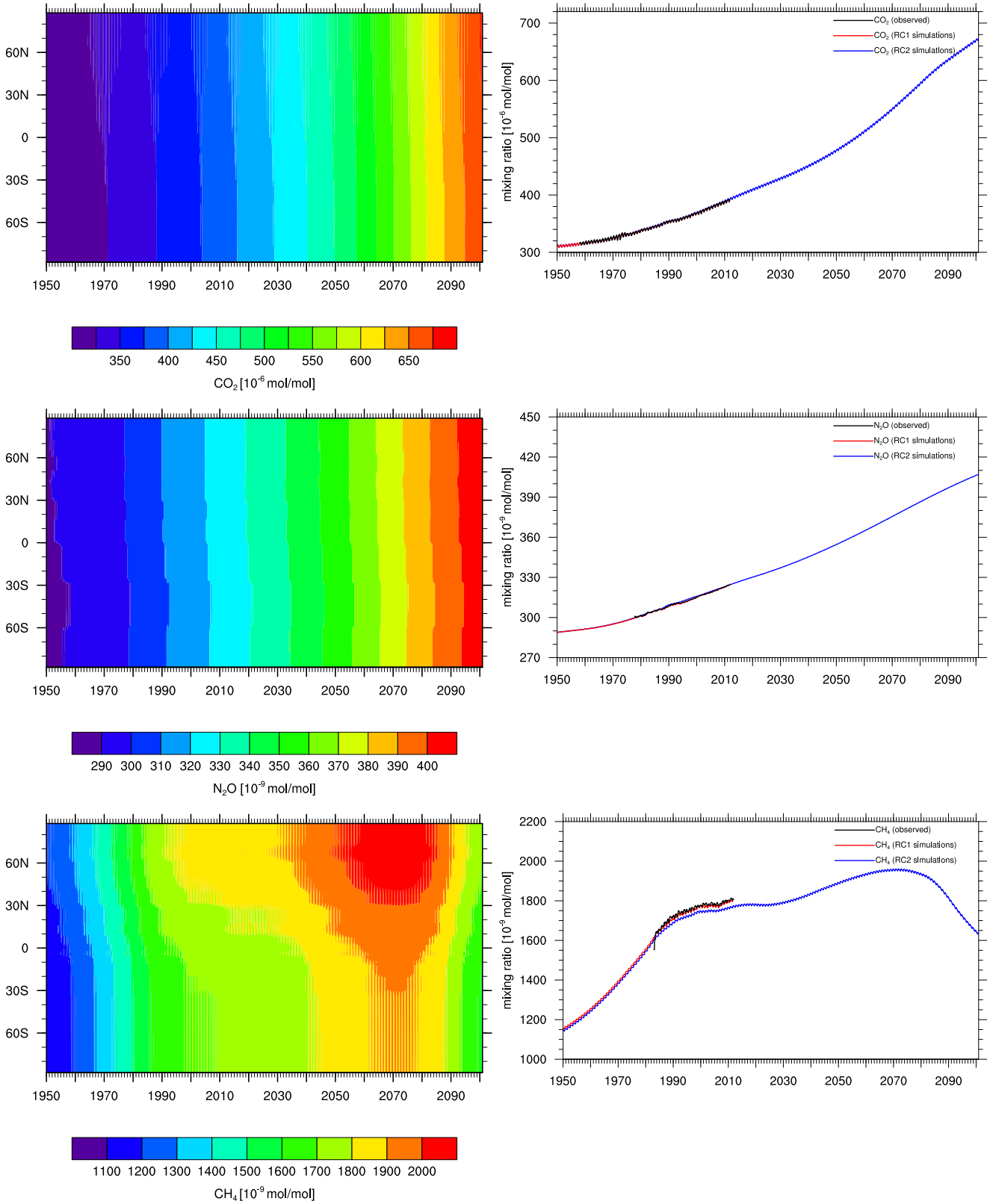

Figure E1: Left column: Time series of latitude dependent CO_2 (top), N_2O (mid) and CH_4 (bottom) as prescribed by Newtonian relaxation in the lowest model layer (shown are only the data used for the *RC2* simulations). Right column: Corresponding globally averaged mixing ratios, prescribed data in red (for *RC1* simulations) and blue (for *RC2* simulations) compared to observations (black). Corresponding data files are DLR_1.0_X_sfmr_GHG_195001-201112.nc (*RC1*) and CCMI_DLR1.0_RCP6.0_sfmr_GHG_195001-210012.nc, respectively.

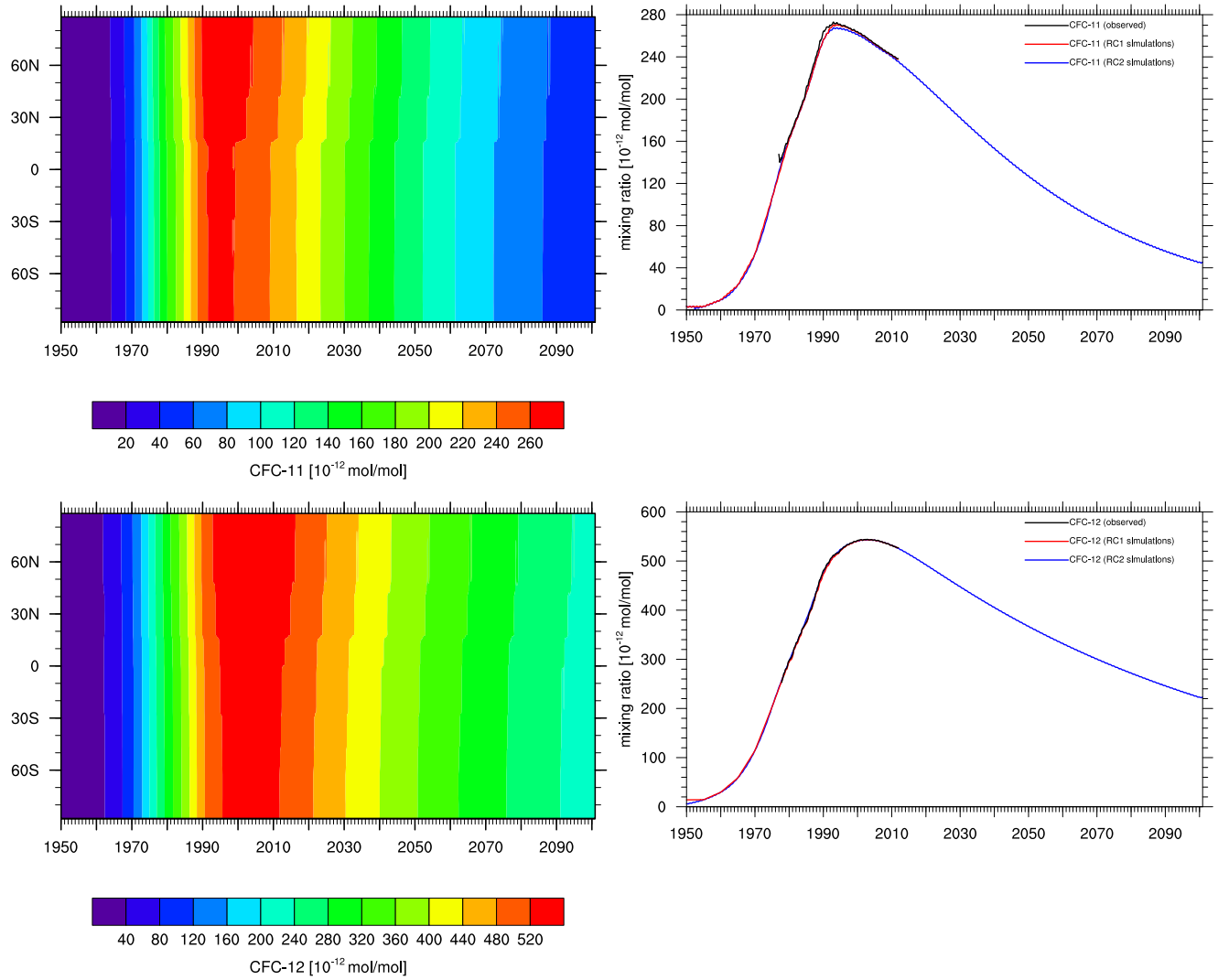

Figure E2: Same as Figure E1, but for the CFCs CFC-11 ($CFCl_3$, top) and CFC-12 (CF_2Cl_2, bottom). Corresponding data files are DLR_1.0_X_sfmr_CFC_195001-201112.nc (*RC1*) and CCMI_DLR1.0_RCP6.0_sfmr_CFC_195001-210012.nc (*RC2*), respectively.

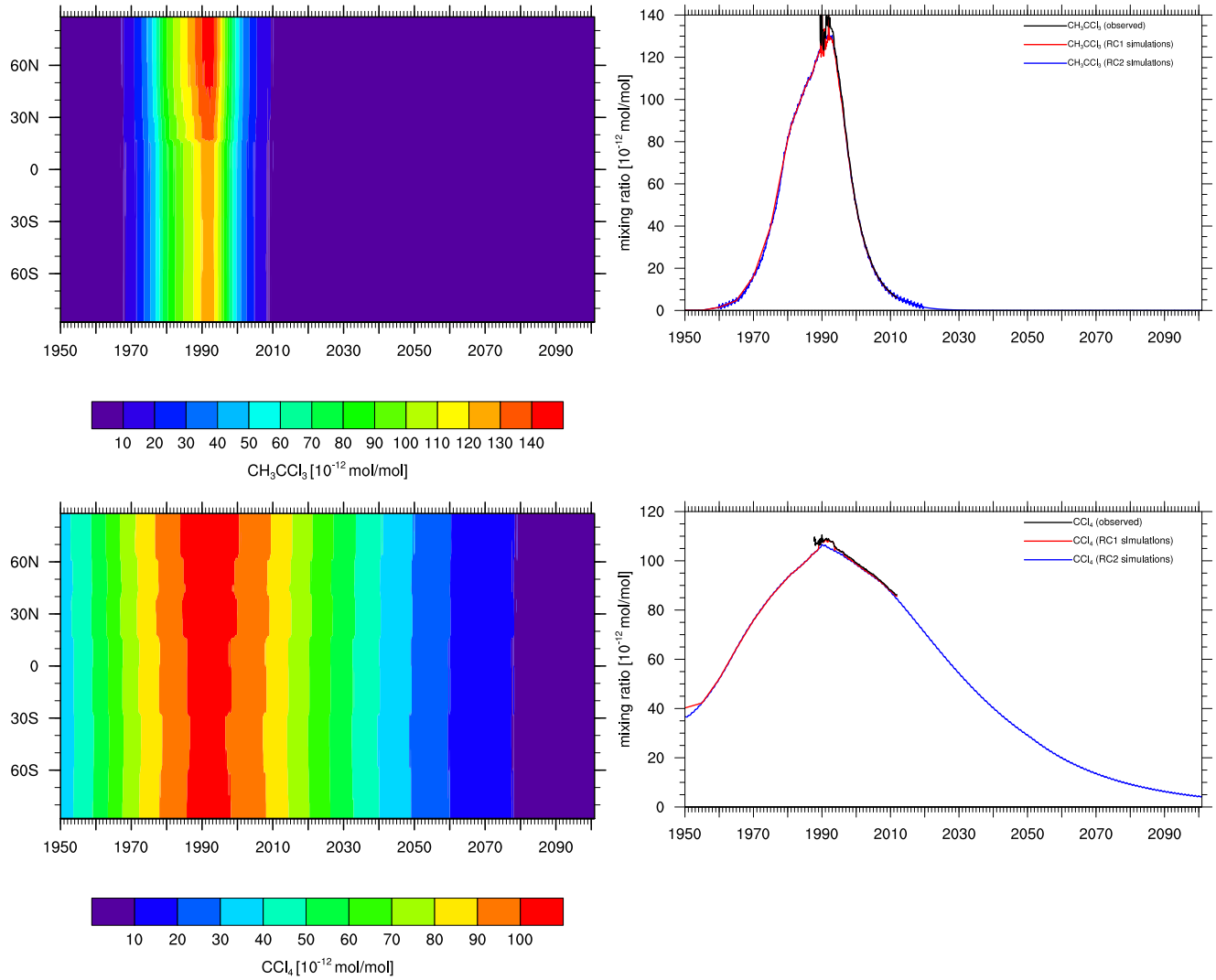

Figure E3: Same as Figure E1, but for the CFCs CH_3CCl_3 (top) and CCl_4 (bottom). Corresponding data files are DLR_1.0_X_sfmr_CFC_195001-201112.nc (*RC1*) and CCMI_DLR1.0_RCP6.0_sfmr_CFC_195001-210012.nc (*RC2*), respectively.

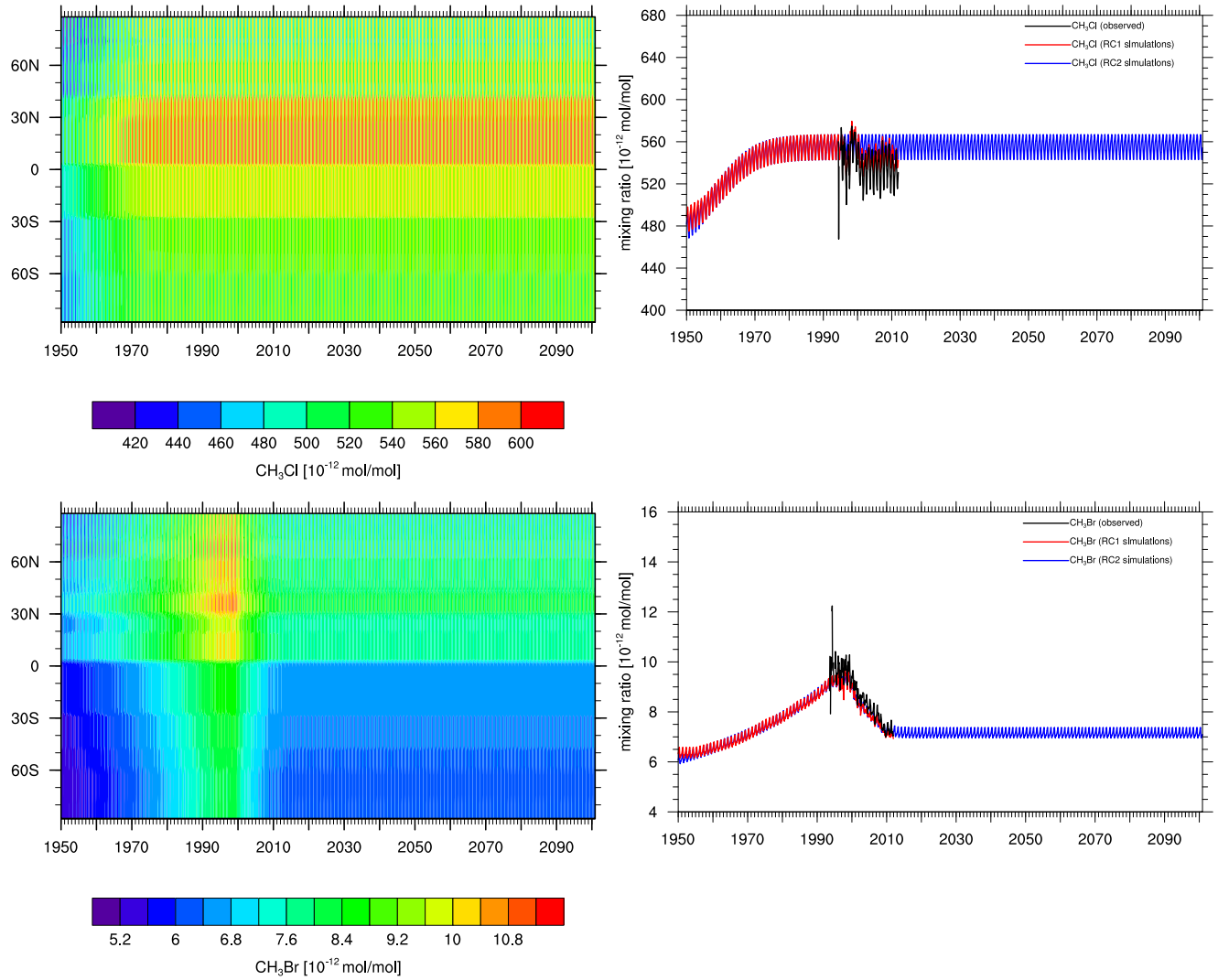

Figure E4: Same as Figure E1, but for the HCFCs CH_3Cl (top) and CH_3Br (bottom). Corresponding data files are DLR_1.0_X_sfmr_HCFC_195001-201112.nc (*RC1*) and CCMI_DLR1.0_RCP6.0_sfmr_HCFC_195001-210012.nc (*RC2*), respectively.

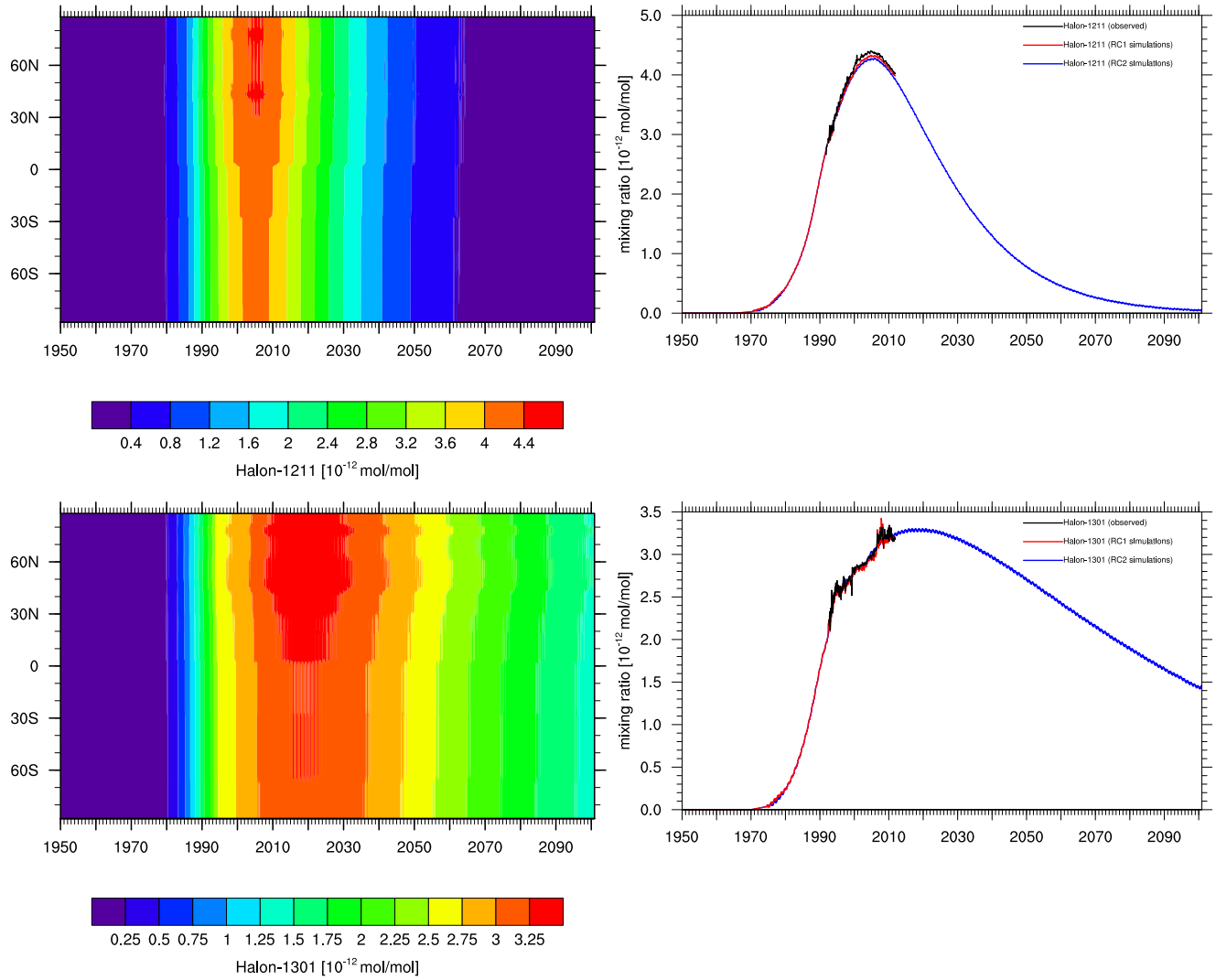

Figure E5: Same as Figure E1, but for the Halons Halon-1211 (CF_2ClBr, top) and Halon-1301 (CF_3Br, bottom). Corresponding data files are DLR_1.0_X_sfmr_Halons_195001-201112.nc (*RC1*) and CCMI_DLR1.0_RCP6.0_sfmr_Halons_195001-210012.nc (*RC2*), respectively.

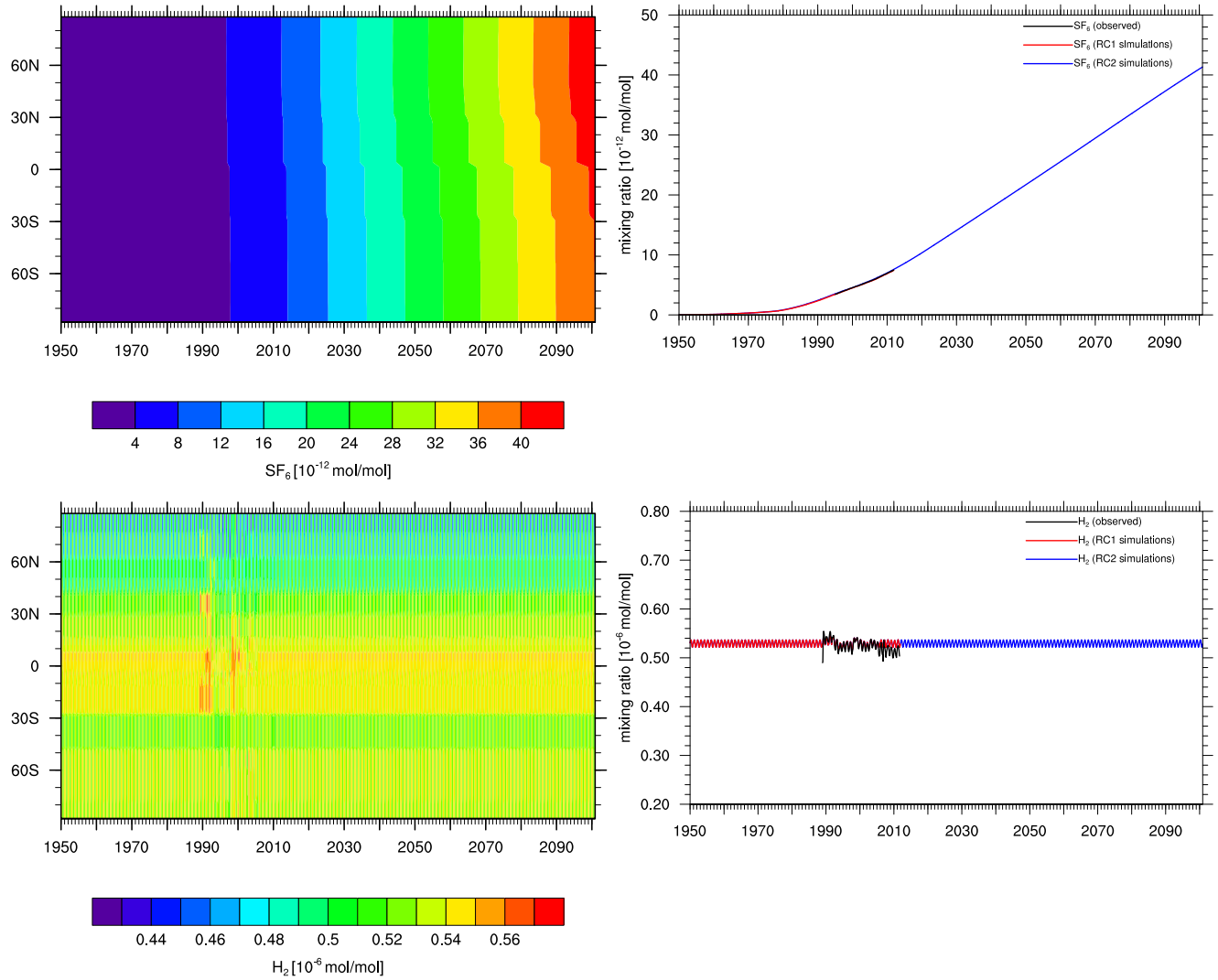

Figure E6: Same as Figure E1, but for SF_6 (top) and H_2 (bottom). Corresponding data files are DLR_1.0_X_sfmr_H2_195001-201112.nc and, CCMI_DLR1.0_RCP6.0_sfmr_SF6_195001-210012.nc for both, *RC1* and *RC2*, respectively.

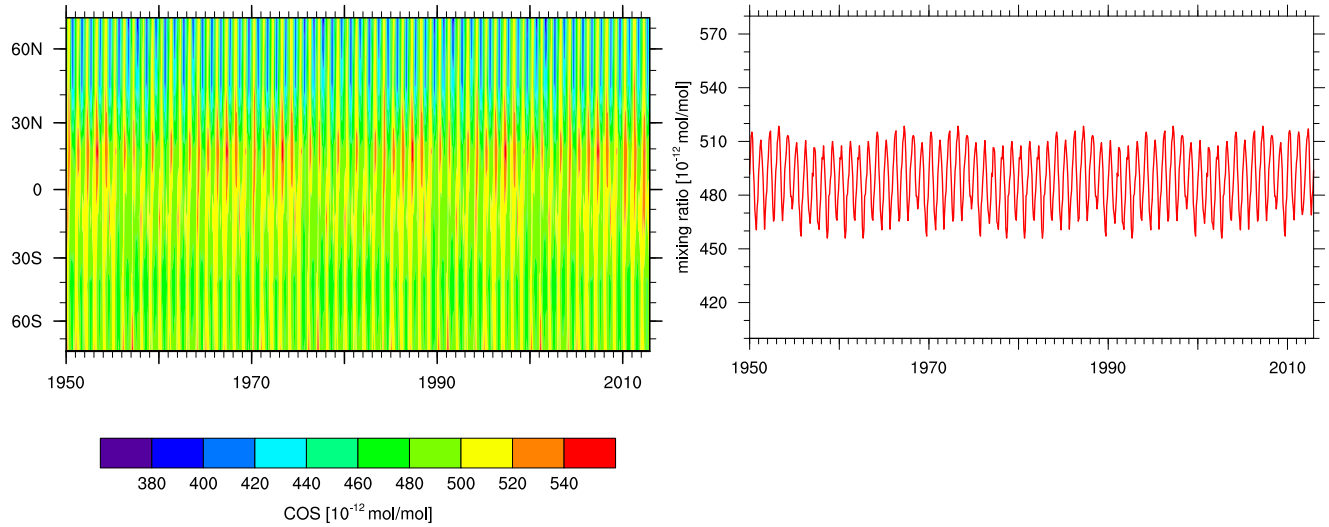

Figure E7: Time series of latitude dependent COS as prescribed in the *RC1-aero* and *RC1-aecl* simulations by Newtonian relaxation in the lowest model layer according to Brühl et al. (2012). The corresponding data file is MPIC_UMZ1.0_X_sfmr_COS_195001-201212.nc.

3 Prescribed boundary conditions for spin-up simulations with coupled ocean model

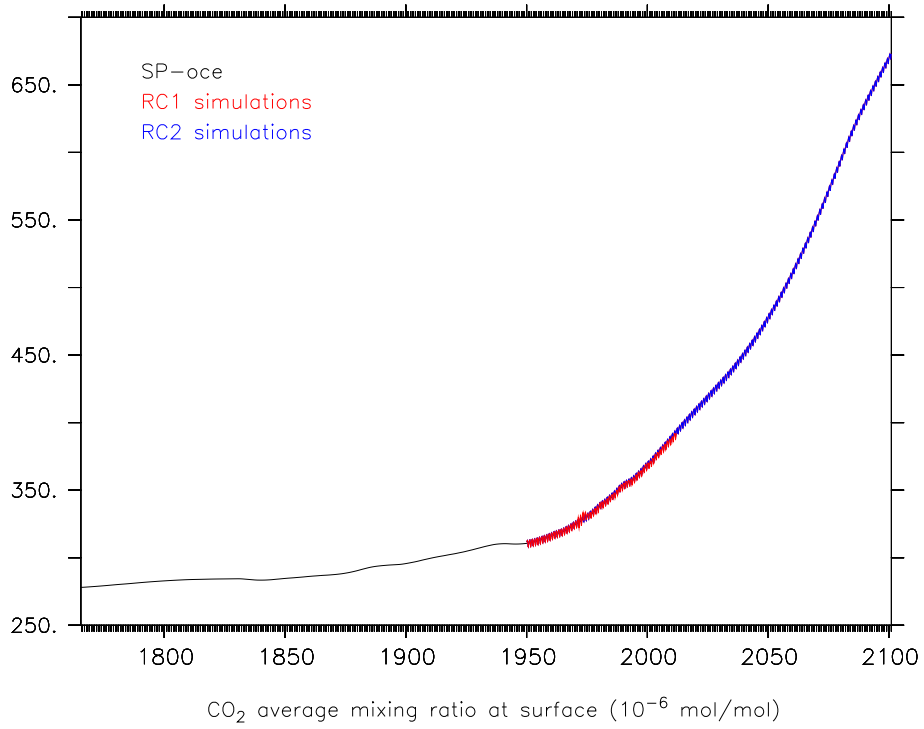

Figure E8: Time series of CO_2 mixing ratio as prescribed for the ocean spin-up simulation *SP-oce-02* (black) in comparison to the time series prescribed for the *RC1* (red) and *RC2* (blue) simulations.

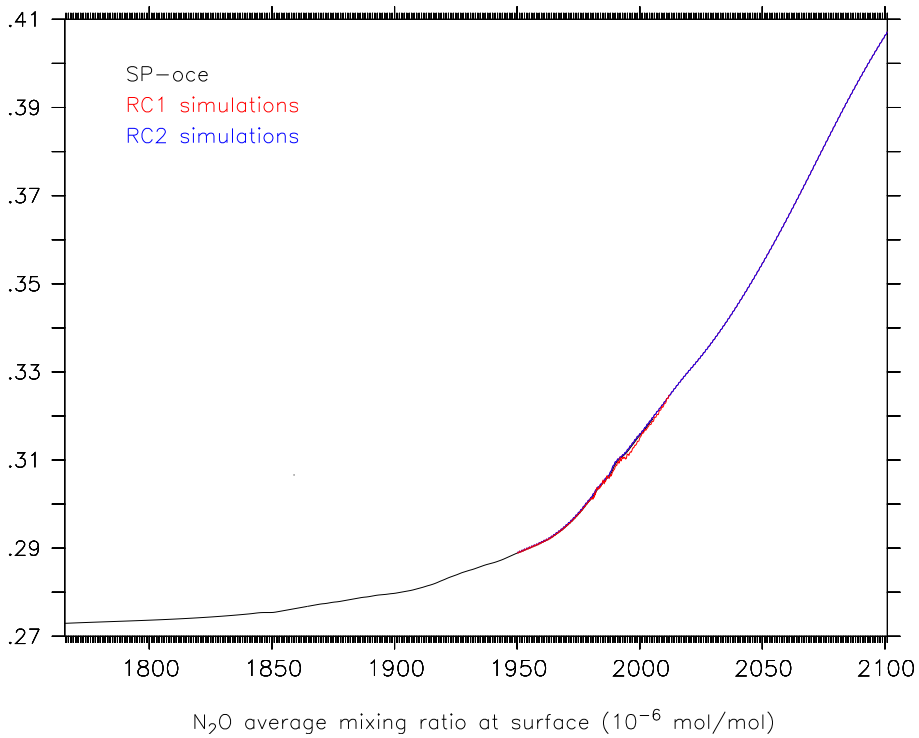

Figure E9: As Figure E8, but for N_2O.

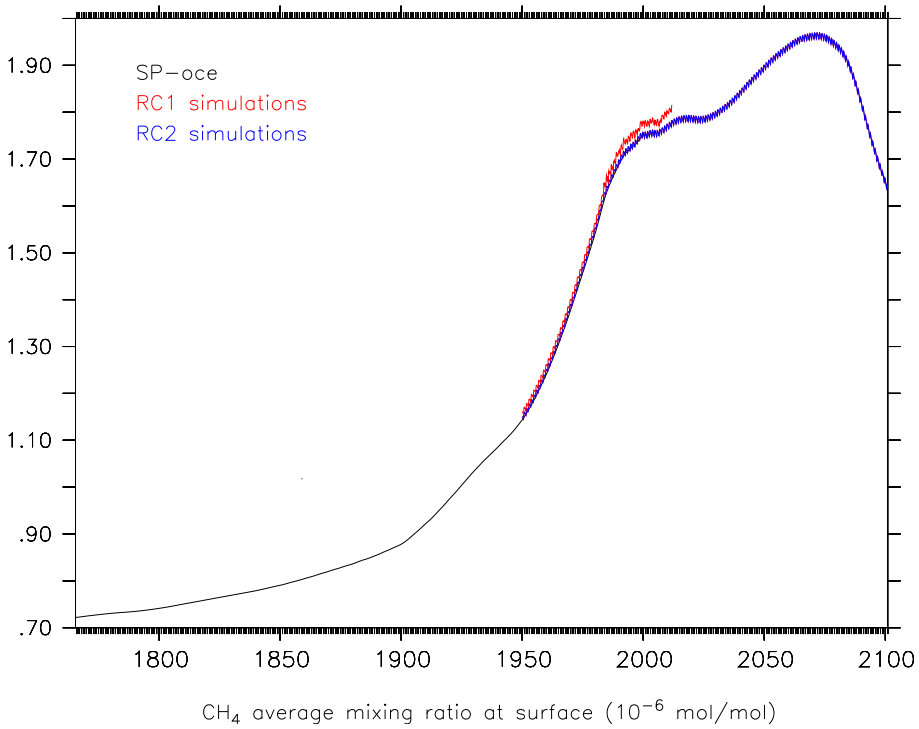

Figure E10: As Figure E8, but for CH_4.

4 Prescribed anthropogenic emissions

4.1 Naming conventions

The anthropogenic emission sectors used throughout this document are defined as:

land:

- emissions from agricultural production (source categories 4A, 4B, 4C, 4D and 4G as defined in the "2006 IPCC guidelines for national greenhouse gas inventories"[1])
- emissions from residential and commercial combustion (source categories 1A4a, 1A4b and 1A4c)
- emission from energy production and distribution (source categories 1A1 and 1B)
- emissions from industrial processes and combustion (source categories 1A2, 2A, 2B, 2C, 2D and 2G)
- emissions from solvent production and use (source categories 2F and 3)
- emissions from waste treatment and disposal (source categories 6A, 6B, 6C and 6D)

awb: emissions from agricultural waste burning (source categories 1A4a, 1A4b and 1A4c)

air: emissions from aviation (aircraft, source category 1A3a)

road: emissions from land transport (source categories 1A3b, 1A3c and 1A3e)

ship: emissions from maritime transport (source category 1A3d)

Two different emission inventories have been preprocessed and used for the ESCiMo simulations, the data are stored in netCDF[2] files:

MACCity (used for the RC1 and RC1SD simulations):

```
CCMI_DLR1.0_AR5-RCP8.5_air_BC_195001-201012.nc
CCMI_DLR1.0_AR5-RCP8.5_air_NOx_195001-201012.nc
CCMI_DLR1.0_AR5-RCP8.5_awb_aerosol_195001-201012.nc
CCMI_DLR1.0_AR5-RCP8.5_awb_MISC_195001-201012.nc
CCMI_DLR1.0_AR5-RCP8.5_land-road-awb_aerosol_195001-201012.nc
CCMI_DLR1.0_AR5-RCP8.5_land-road-awb_MISC_195001-201012.nc
CCMI_DLR1.0_AR5-RCP8.5_road_aerosol_195001-201012.nc
CCMI_DLR1.0_AR5-RCP8.5_road_MISC_195001-201012.nc
CCMI_DLR1.0_AR5-RCP8.5_ship_aerosol_195001-201012.nc
CCMI_DLR1.0_AR5-RCP8.5_ship_MISC_195001-201012.nc
CCMI_DLR1.0_REFC1_bb_aerosol_195001-201012.nc
CCMI_DLR1.0_REFC1_bb_MISC_195001-201012.nc
CCMI_DLR1.0_REFC1_bb_NMHC_195001-201012.nc
```

ACCMIP+AR5/RC6.0 (used for the RC2 simulations):

```
CCMI_DLR1.0_AR5-RCP6.0_air_BC_195001-210012.nc
CCMI_DLR1.0_AR5-RCP6.0_air_MISC_195001-210012.nc
CCMI_DLR1.0_AR5-RCP6.0_anth_MISC_195001-210012.nc
CCMI_DLR1.0_AR5-RCP6.0_awb_MISC_195001-210012.nc
CCMI_DLR1.0_AR5-RCP6.0_bb_MISC_195001-210012.nc
CCMI_DLR1.0_AR5-RCP6.0_bb_NMHC_195001-210012.nc
CCMI_DLR1.0_AR5-RCP6.0_land-road-awb_MISC_195001-210012.nc
CCMI_DLR1.0_AR5-RCP6.0_road_MISC_195001-210012.nc
CCMI_DLR1.0_AR5-RCP6.0_ship_MISC_195001-210012.nc
(CCMI_DLR1.0_AR5-RCP6.0_awb_aerosol_195001-210012.nc)
```

[1] http://www.ipcc-nggip.iges.or.jp/public/2006gl/
[2] http://www.unidata.ucar.edu/software/netcdf/

```
(CCMI_DLR1.0_AR5-RCP6.0_bb_aerosol_195001-210012.nc)
(CCMI_DLR1.0_AR5-RCP6.0_land-road-awb_aerosol_195001-210012.nc)
(CCMI_DLR1.0_AR5-RCP6.0_road_aerosol_195001-210012.nc)
(CCMI_DLR1.0_AR5-RCP6.0_ship_aerosol_195001-210012.nc)
```

Files in parentheses have not been used in the present simulations, but are shown for completeness (see also Section 4.3).

4.2 Description of the inventories

4.2.1 MACCity

MACCity is a global emission inventory with a resolution of 0.5^o x 0.5^o. The files contain monthly emissions for the years 1950 - 2010. Starting in 2000 the data set is based on the "MACCity" emissions (see Granier et al. (2011)), followed by the IPCC AR5 RCP8.5 scenario for 2005 and 2010. The data were downloaded from the ECCAD-Website (`http://eccad.sedoo.fr/`) for anthropogenic emissions and from `ftp://ftp-ipcc.fz-juelich.de` for the biomass burning emissions. They contain the emissions from the following sectors:

- land (without awb and road)
- road
- awb
- air(craft)
- ship
- biomass burning

The MACCity inventory is based on the ACCMIP emission inventory described by Lamarque et al. (2010). The data of the years 1960, 1970, 1980, 1990, 2000, 2005 and 2010 were linearly interpolated. Additionally, a seasonal cycle was applied, more precisely sector-specific cycles were used as developed for the RETRO project (Schultz et al., 2007). In the MACCity dataset the ACCMIP non-methane hydrocarbon (NMHC) species were lumped into 21 species. Despite the detailed documentation on the ECCAD web-site, no detailed information about the lumping of the species was available. As this lumped species are not compatible with the chemical mechanism used in MECCA, the data needed to be preprocessed. Details about this are documented in Section 4.2.3 and in Figure E11.

The emissions of the different sectors were distributed to different height levels according to Pozzer et al. (2009). As the MACCity data does not contain emissions for the year 1950, the emissions of the year 1960 have been used for the years 1950 - 1959.

4.2.2 ACCMIP+AR5/RCP6.0

The ACCMIP+AR5/RCP6.0 inventory is a global emissions inventory for the years 1950-2100. It contains monthly data (without seasonal variability) with a resolution of 0.5^ox0.5^o. The sectors available are:

- land (without awb and road)
- road
- awb
- air(craft)
- ship
- biomass burning

The data were downloaded from `ftp://ftp-ipcc.fz-juelich.de` and then linearly interpolated from the ACCMIP inventory for the years 1950 - 2000. After the year 2000 the emissions from the RCP6.0 scenario are used, which were linearly interpolated, too. The emissions of the different sectors were distributed to different height levels according to Pozzer et al. (2009).

4.2.3 Notes on the NMHC emissions

The ACCMIP+AR5/RCP6.0 raw data contain a "total NMHC" species for each sector. For MECCA these totals have been converted from kg(NMHC) to kg(C) and subsequently split into the individual species following the speciation suggested by von Kuhlmann et al. (2003). The conversion from kg(NMHC) to kg(C) was achieved by scaling with a factor of 161/210 according to IPCC (2001, Section 4.2.3.2., Table 4.7.b, see also Hoor et al. (2009)).

The MACCity raw data comprise 21 lumped species, but no "total NMHC" species for the different sectors. However, as mentioned above, it was not documented how the species were lumped. To yield total NMHC, which is required for the MECCA-specific speciation, the total kg(C) of the NMHC emissions from each sector have been calculated as sketched in Figure E11. As a result, the used data files with ACCMIP+AR5/RCP6.0 emissions contain "total NMHC" in kg(NMHC), whereas the MACCity data files contain "total NMHC" in kg(C).

The NMHC biomass burning emissions of both data sets have been processed similarly to the MACCity emissions. From the available lumped species the total emissions in Tg(C) have been calculated, which where then translated to emissions fluxes of the species in the applied chemical mechanism.

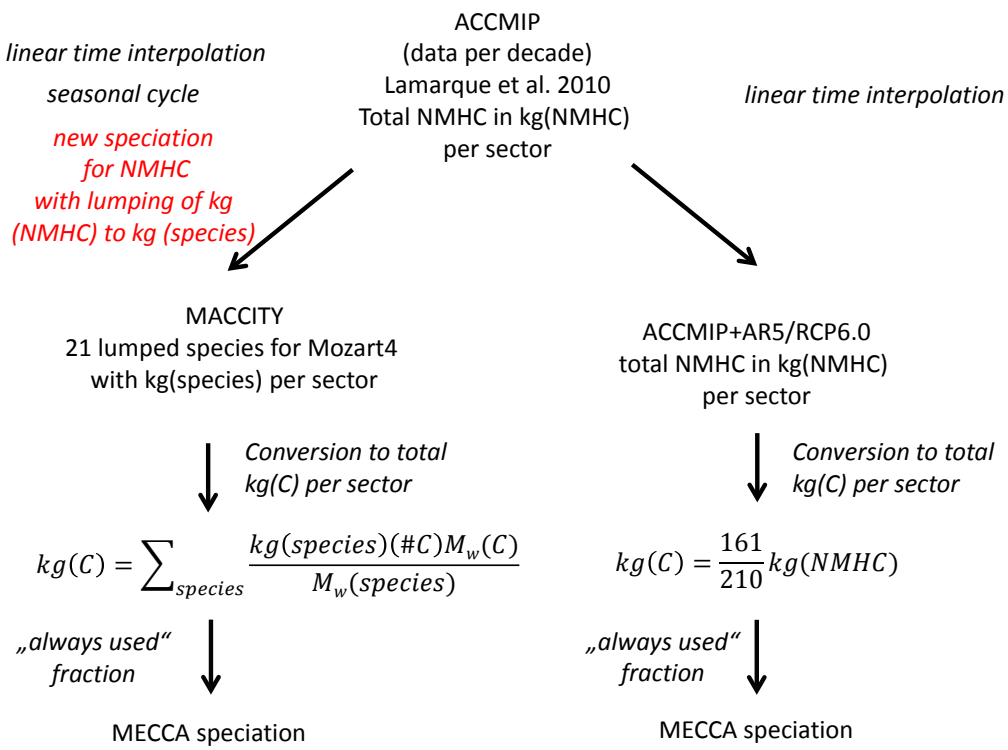

Figure E11: Difference between the NMHC speciation in the MACCity and ACCMIP+AR5/RCP6.0 datasets. While the ACCMIP+AR5/RCP6.0 raw data contain total NMHC values, which could be directly speciated, the MACCity raw data contain different species, but no total NMHC and therefore required a special preprocessing.

4.2.4 Notes on the ACCMIP emissions

The different sectors of the ACCMIP dataset, labelled for a specific decade, correspond to different times: "In the historical decadal ACCMIP emission files, the anthropogenic and aircraft emissions represent the first year of the corresponding decade, while ship emissions represent the 5th year of the corresponding decade. The biomass burning emissions represent average conditions of the corresponding decade (e.g., 1980 - 1989 mean values are contained in the file labelled with year 1980), except for the 2000 estimate, which is calculated from the 1997-2006 average."[3]

[3]source: `ftp://ftp-ipcc.fz-juelich.de/pub/emissions/gridded_netcdf/accmip_interpolated/README.accmip_interpolated.txt`

4.3 Comparison of inventories by sector

This section provides a comparison of the total emissions (for the different sectors) of the different inventories. Totals for NMHC are given in Tg(C)/a; NMHC from the ACCMIP+AR5/RCP6.0 inventory has been converted by scaling with 161/210, whereas NMHC in the MACCity inventory was already in kg(C). Totals for NOx are given in Tg(NO)/a, black (BC) and organic carbon (OC) in Tg(C)/a, all others in Tg(species)/a. Note that emissions of OC and BC have only been used in the *RC1-aero* and *RC1-aecl* simulations. Corresponding emissions of the ACCMIP+AR5/RCP6.0 inventory are only shown for comparison and have not been used within ESCiMo.

4.3.1 Biomass burning

Figures E12 - E18 show the annual total emissions of CO, NOx, SO_2 and NH_3, NMHC, black carbon and organic carbon of the biomass burning sector. A strong inter-annual variability is present in the emissions of the MACCity dataset. This inter-annual variability is not present in the ACCMIP+AR5/RCP6.0 dataset.

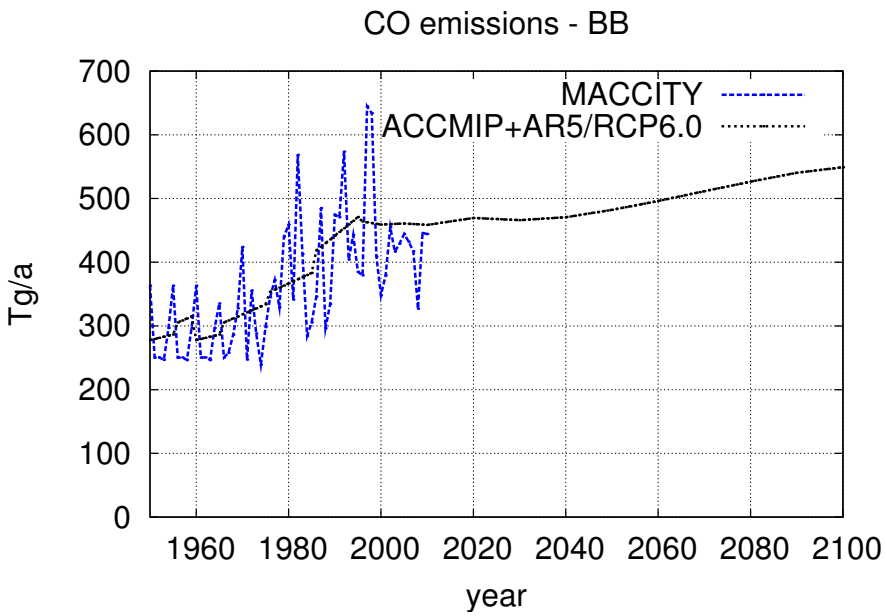

Figure E12: Annual total emissions of CO from the biomass burning sector.

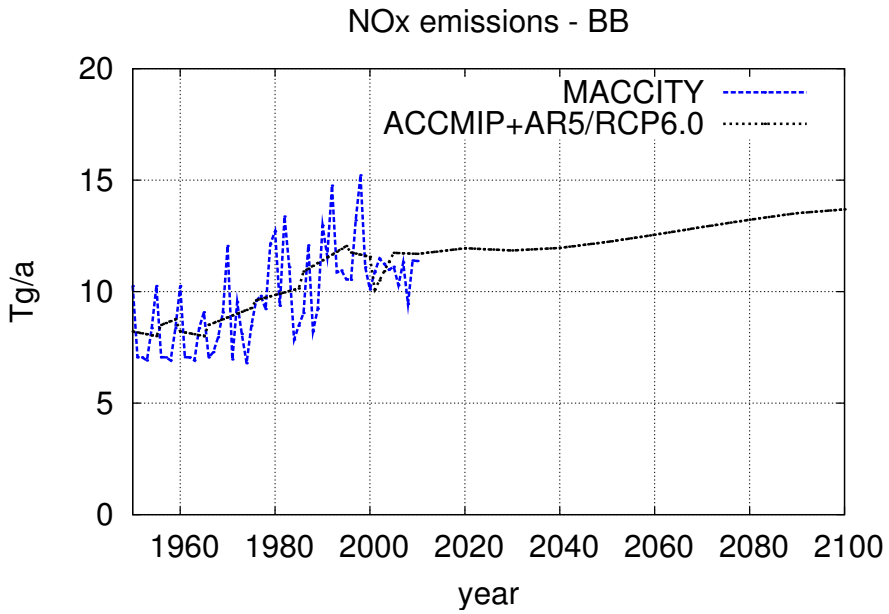

Figure E13: As Figure E12, but for NOx (in Tg(NO)/a).

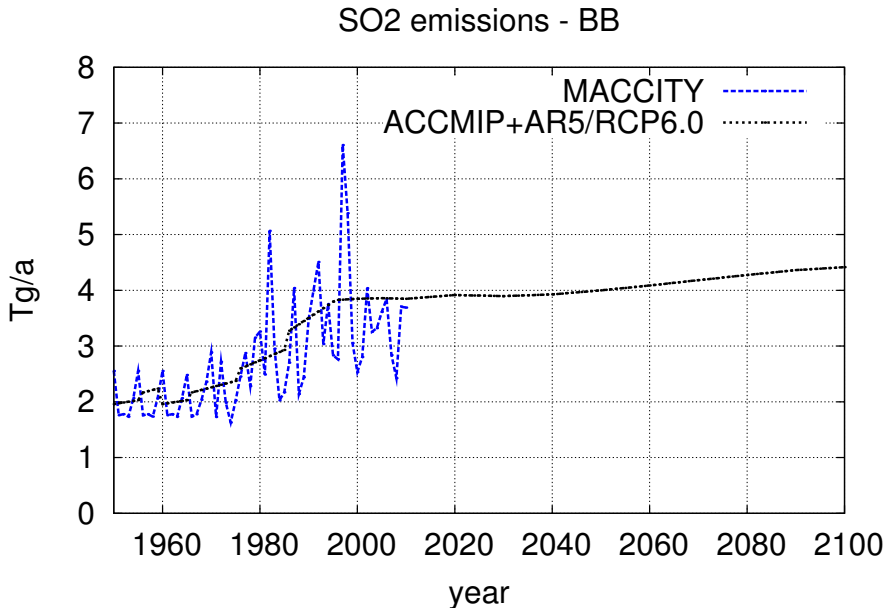

Figure E14: As Figure E12, but for SO_2.

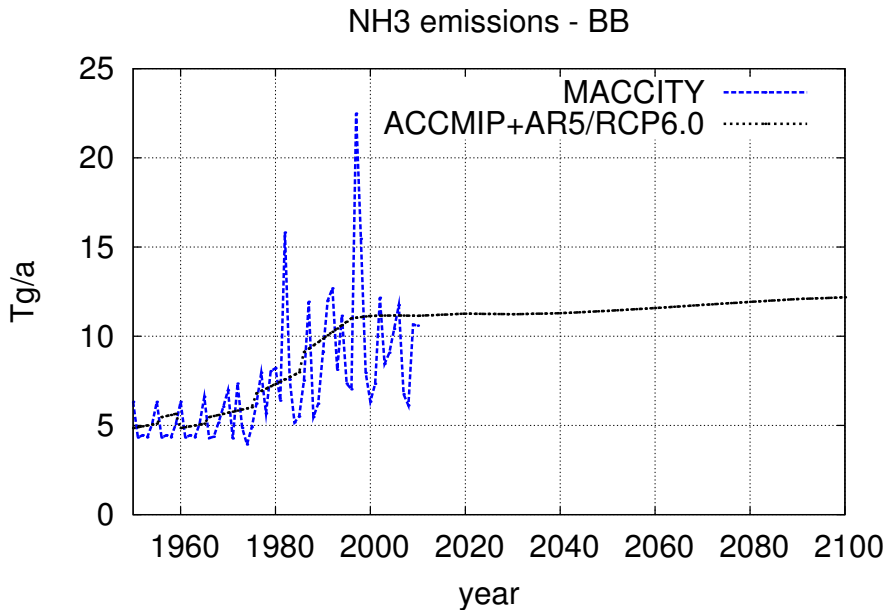

Figure E15: As Figure E12, but for NH_3.

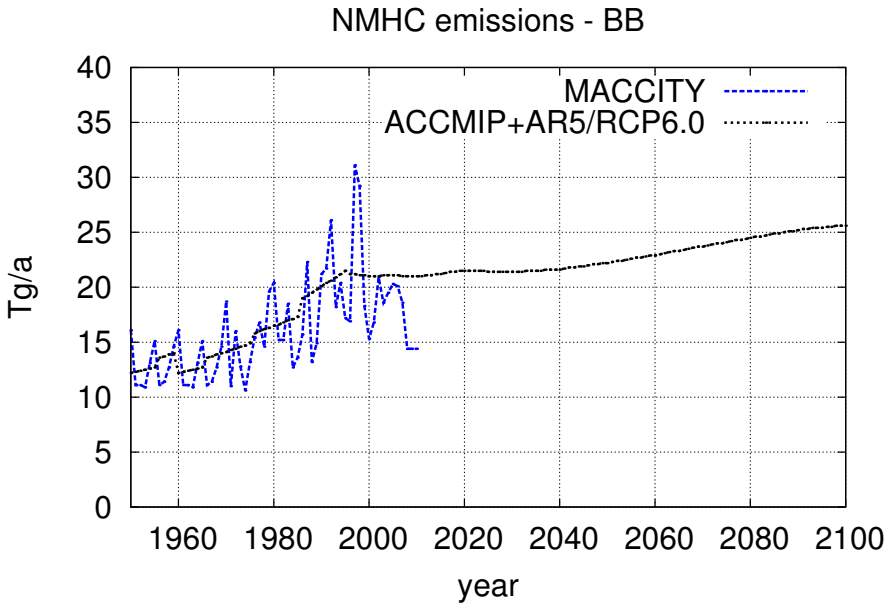

Figure E16: As Figure E12, but for NMHCs (in Tg(C)/a).

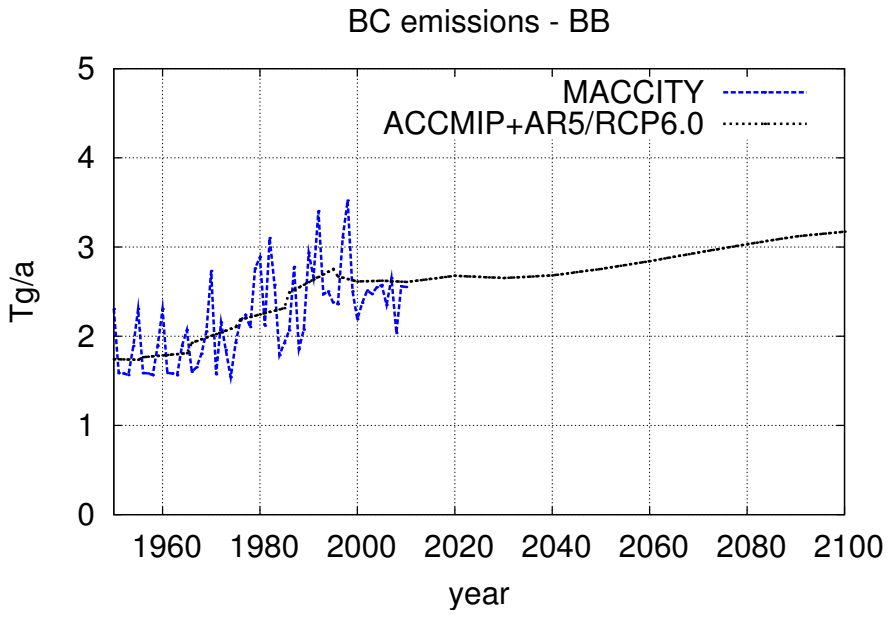

Figure E17: As Figure E12, but for black carbon (in Tg(C)/a).

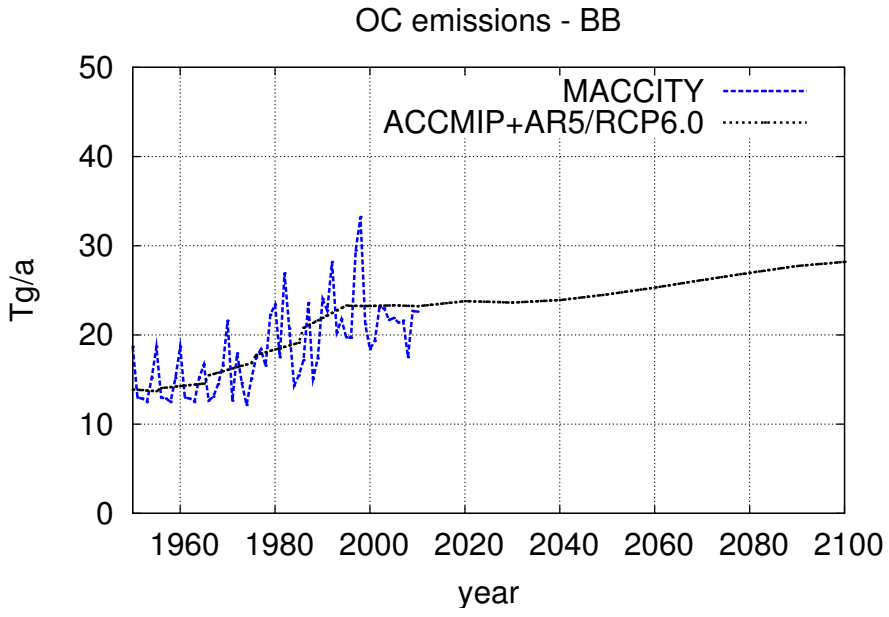

Figure E18: As Figure E12, but for organic carbon (in Tg(C)/a).

4.3.2 Road traffic

Figures E19 - E25 show the annual totals for the years 1950 - 2100 for CO, NOx, SO_2, NH_3, NMHCs, black and organic carbon. The MACCity emissions show no trend for 1950 - 1959 (spin-up phase) by construction. From 1960 on, MACCity and ACCMIP+AR5/RCP6.0 show the same evolution until 2000. Starting 2000, the MACCity dataset follows the AR5 RCP 8.5 pathway, while the ACCMIP+AR5/RCP6.0 follows the RCP6.0 pathway. This is at least true for CO, NOx, SO_2, NH_3, black and organic carbon. For the NMHC emissions (Figure E23) the MACCity emissions are lower than those of ACCMIP+AR5/RCP6.0. Between 1960 and 2010, both inventories are based on the ACCMIP data. Nevertheless, ACCMIP+AR5/RCP6.0 emissions are larger by a factor of about 1.2, corresponding to an absolute difference of up to ∼6 Tg(C)/a. This is presumably an artefact resulting from the different procedure used for the speciation.

Unfortunately there was an error (wrong namelist entry) in the model setup affecting all simulations, except for *RC1SD-base-10a*, the latter having been performed as a sensitivity simulation (in comparison to *RC1-base-10*) to assess the impact of this mistake. The wrong namelist entry caused a wrong timing of the road traffic emissions: Instead of updating the emission distributions from the monthly time series every month, they have been updated only every year. The resulting wrong time series of the road traffic emission are labelled "wrong" in all figures (red line for MACCity, green line for ACCMIP+AR5/RCP6.0).

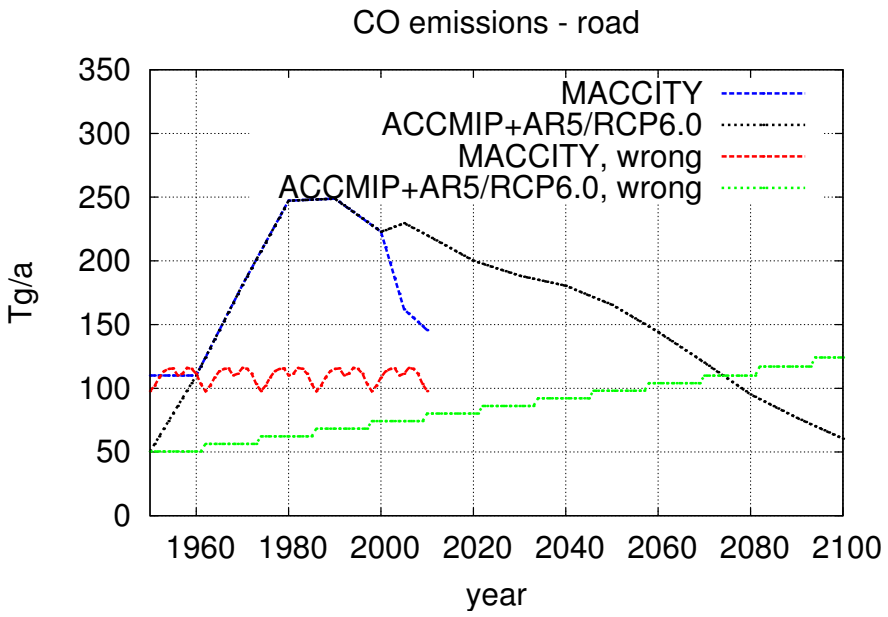

Figure E19: Annual total emissions of CO from the road sector. The two time-lines marked "wrong" show the temporal evolution of the emissions as wrongly applied in all model simulations (except for *RC1SD-base-10a)* as a result of an error in the model setup.

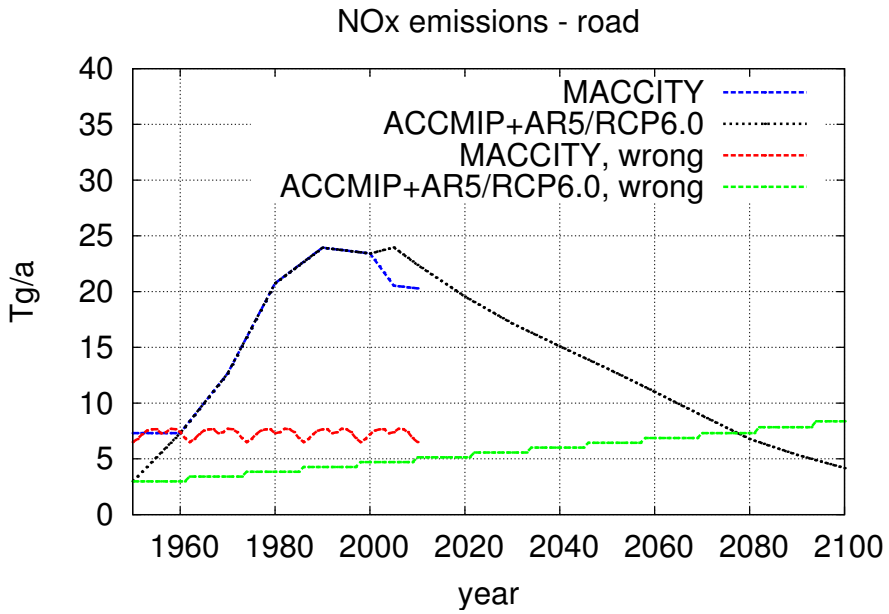

Figure E20: As Figure E19, but for NOx (in Tg(NO)/a).

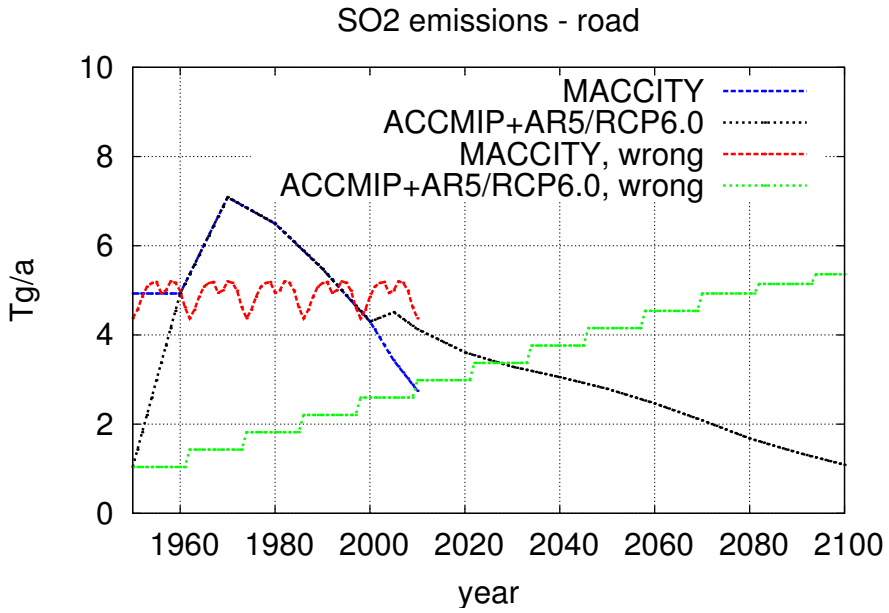

Figure E21: As Figure E19, but for SO_2.

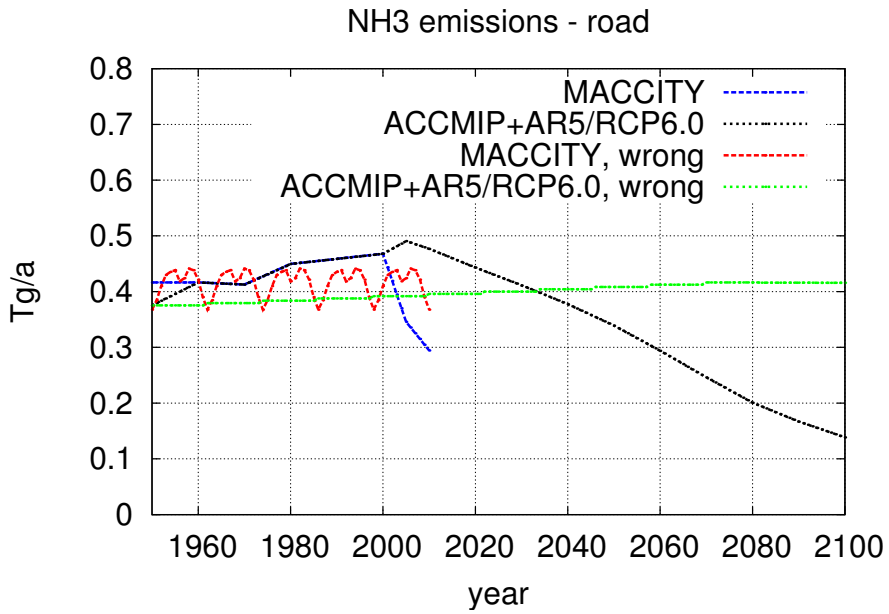

Figure E22: As Figure E19, but for NH_3.

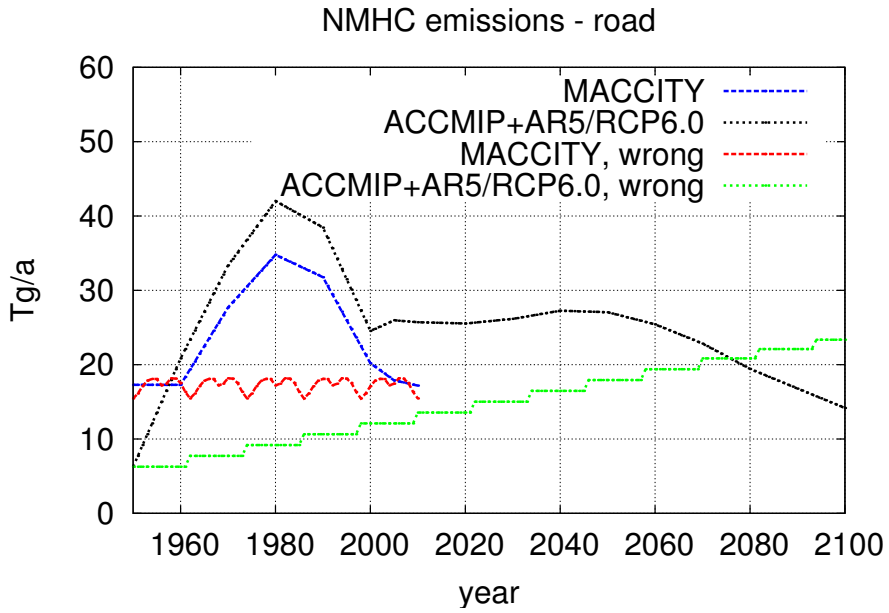

Figure E23: As Figure E19, but for NMHC (in Tg(C)/a).

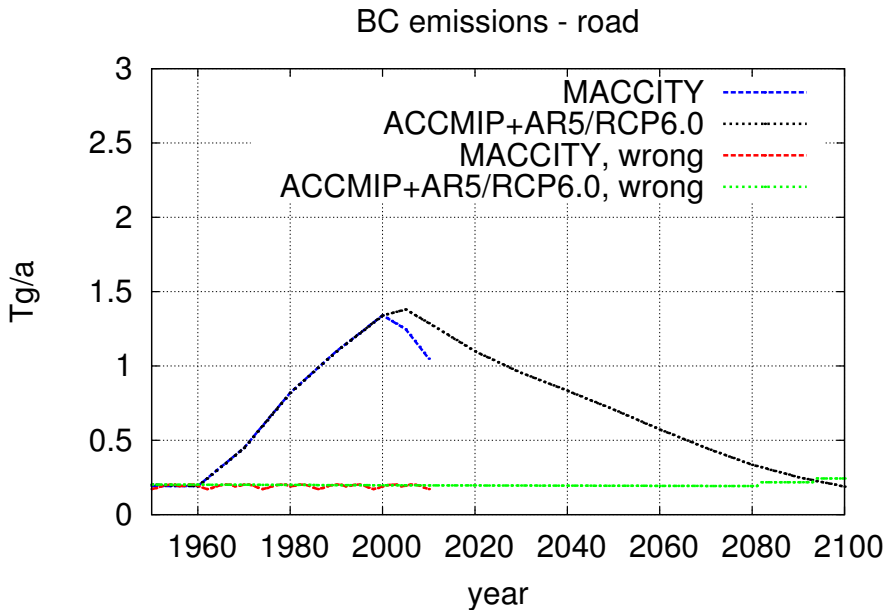

Figure E24: As Figure E19, but for black carbon (in Tg(C)/a).

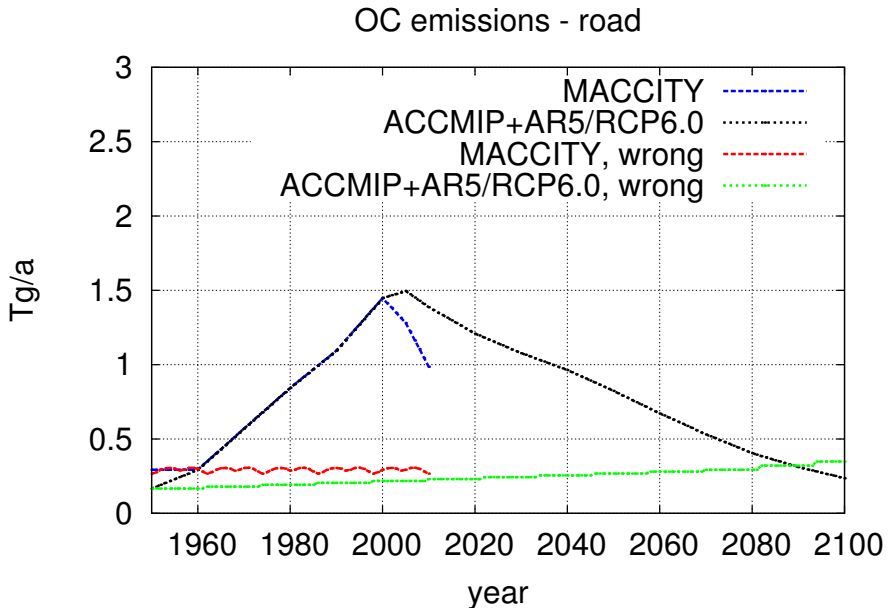

Figure E25: As Figure E19, but for organic carbon (in Tg(C)/a).

4.3.3 Agricultural waste burning

Figures E26 - E32 show the annual totals for the years 1950 - 2100 for CO, NOx, SO_2, NH_3, NMHC, black and organic carbon. As above, CO, NOx, SO_2, NH_3, black and organic carbon are identical from 1960 - 2000. Once again, the total emissions of NMHC in the MACCity and ACCMIP+AR5/RCP6.0 data differ between 1960 and 2010 by around 1 Tg(C)/a (see Figure E30).

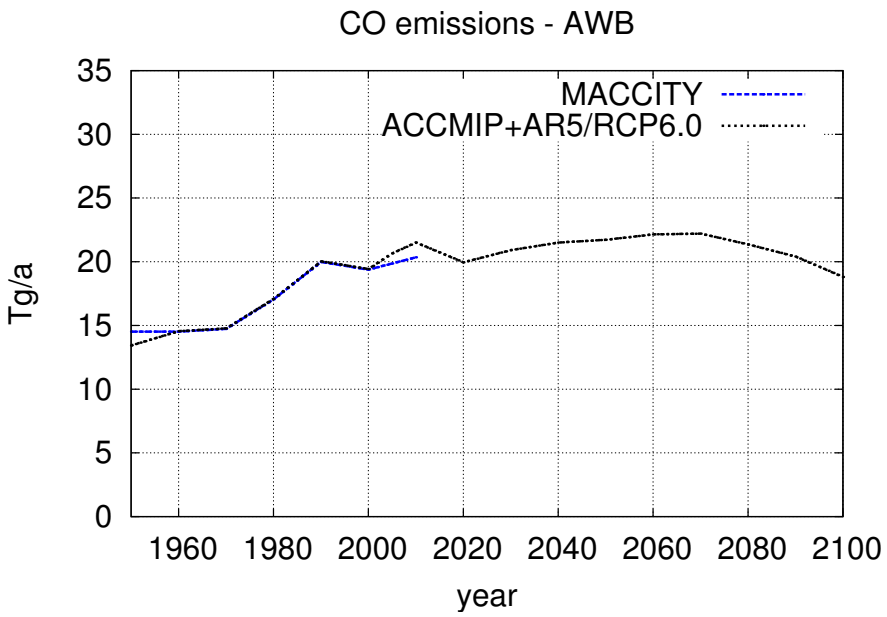

Figure E26: Annual total emissions of CO from the awb sector.

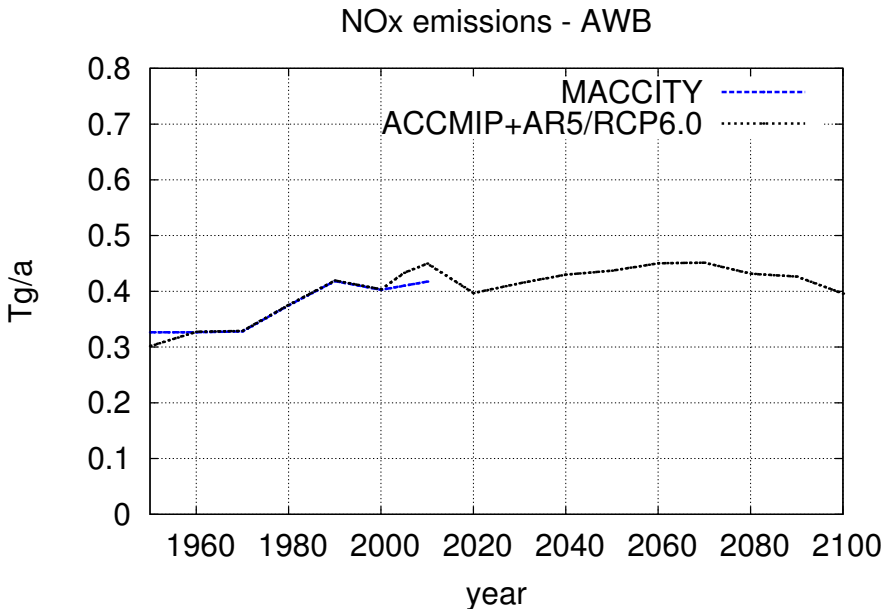

Figure E27: As Figure E26, but for NOx (in Tg(NO)/a).

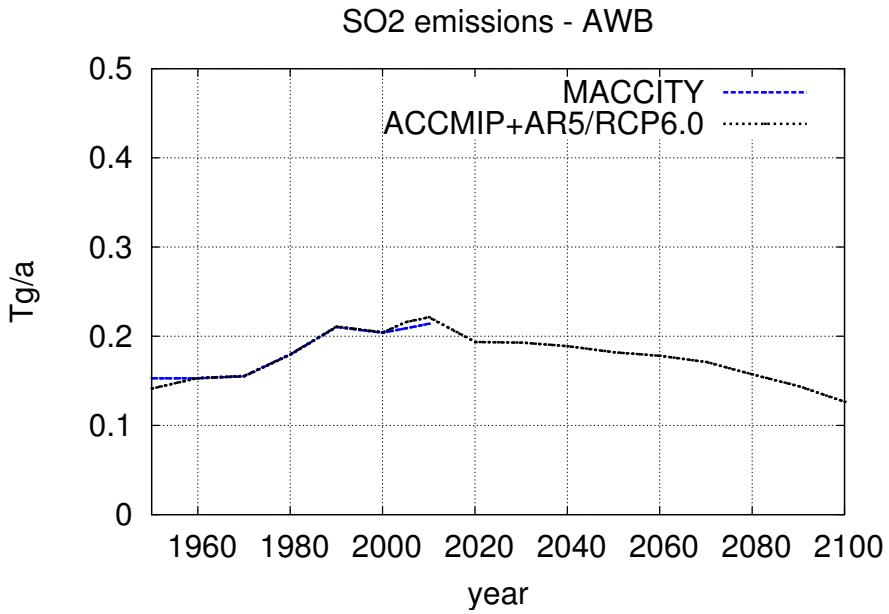

Figure E28: As Figure E26, but for SO_2.

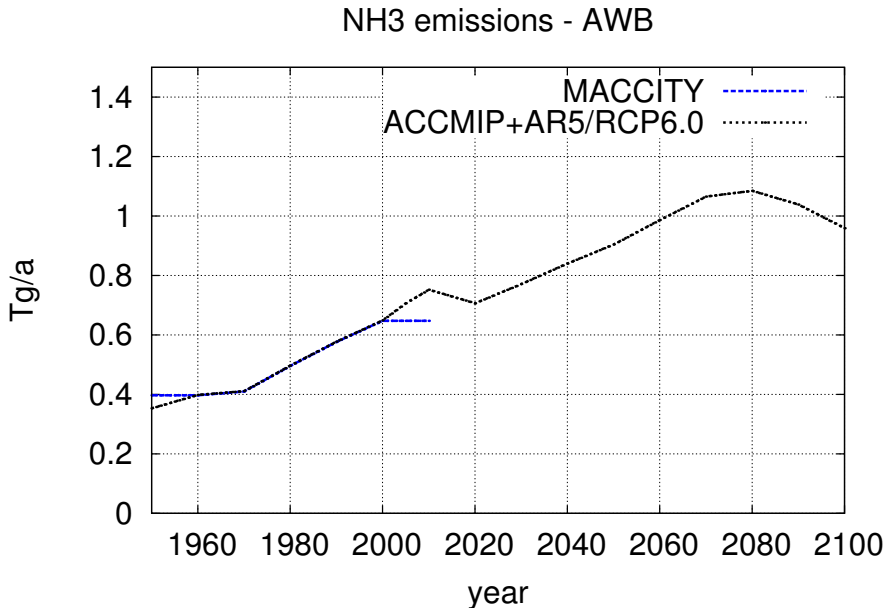

Figure E29: As Figure E26, but for NH_3.

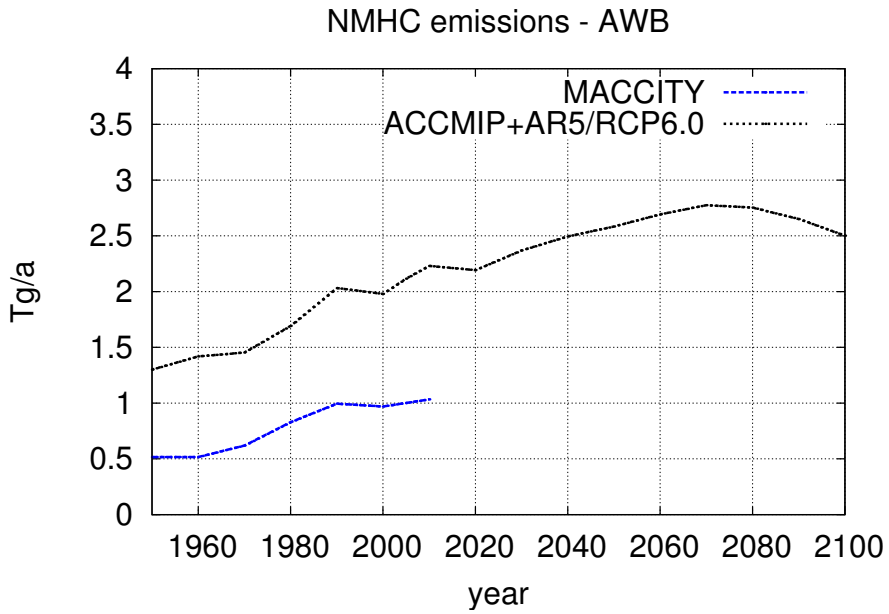

Figure E30: As Figure E26, but for NMHC (in Tg(C)/a).

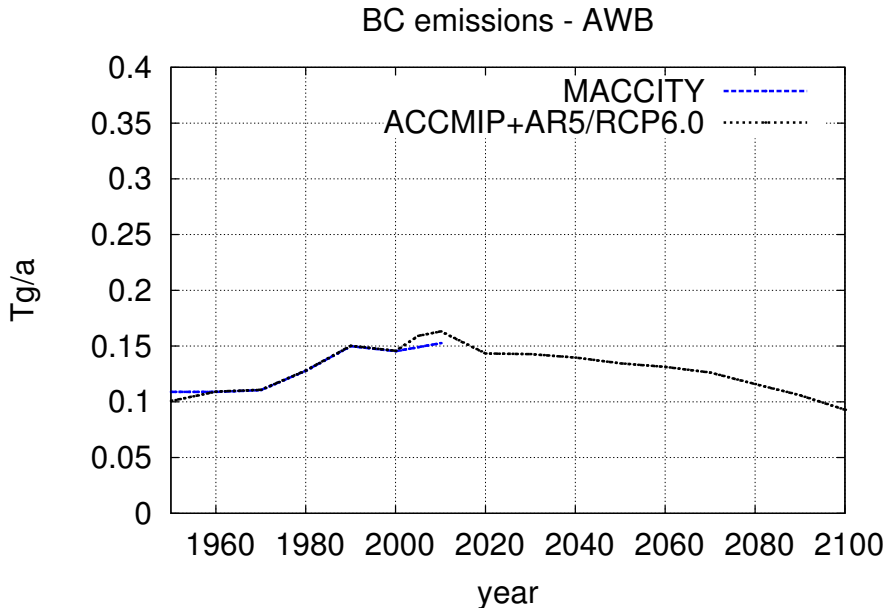

Figure E31: As Figure E26, but for black carbon (in Tg(C)/a).

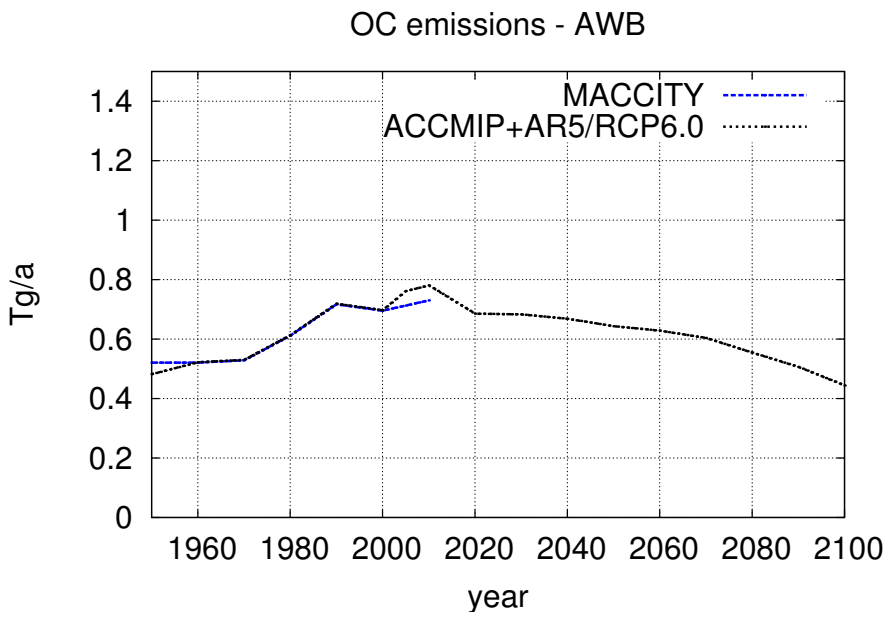

Figure E32: As Figure E26, but for organic carbon (in Tg(C)/a).

4.3.4 Shipping

The annual total emissions of CO, NOx, SO_2, NMHC, black and organic carbon from shipping (Figures E33 - E38) differ between both inventories in the years 1950 - 1999. The reason are the different reference times (shifted by 5 years) as noted above. The NMHC emissions (Figure E36) are about 10% lower in MACCity compared to the ACCMIP+AR5/RCP6.0 estimate.

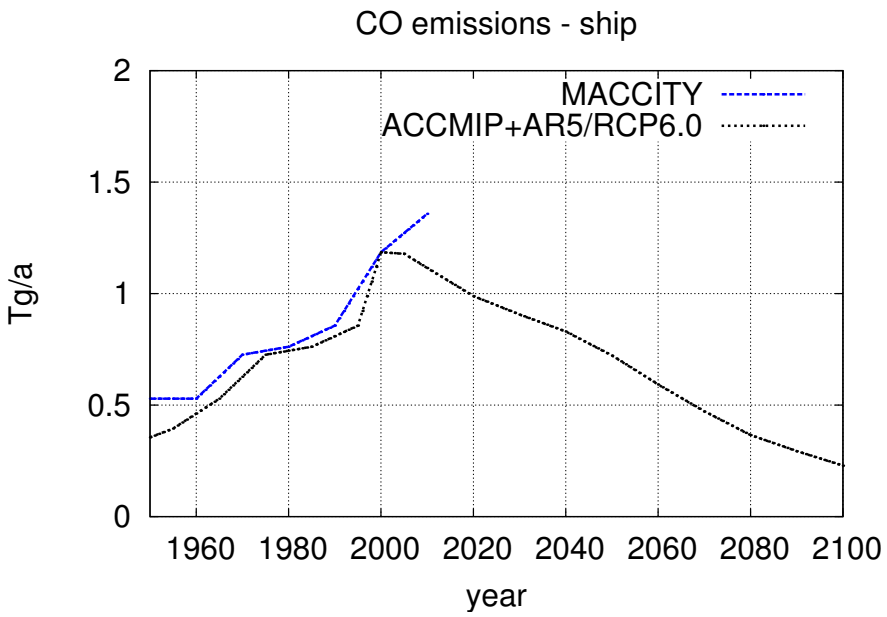

Figure E33: Annual total emissions of CO from the ship sector.

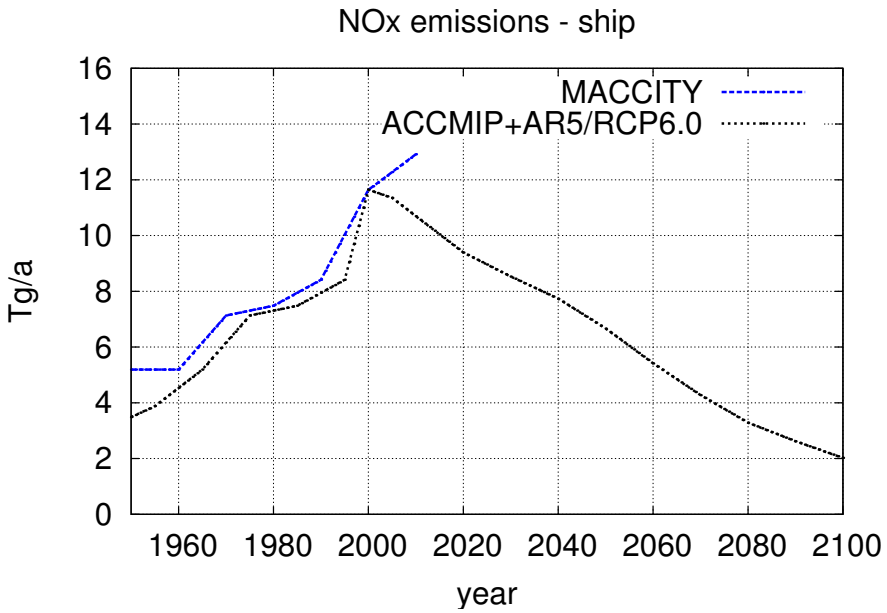

Figure E34: As Figure E33, but for NOx (in Tg(NO)/a).

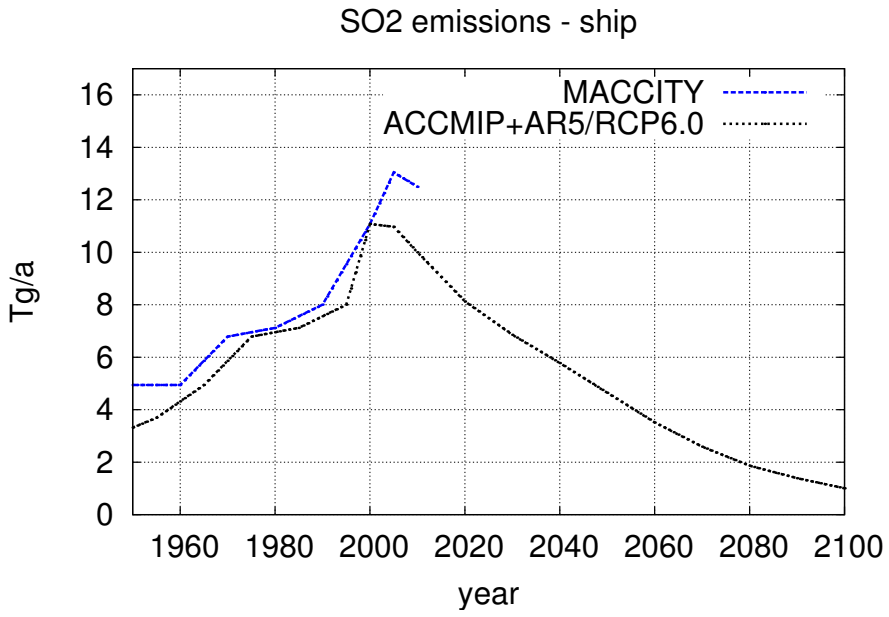

Figure E35: As Figure E33, but for SO_2.

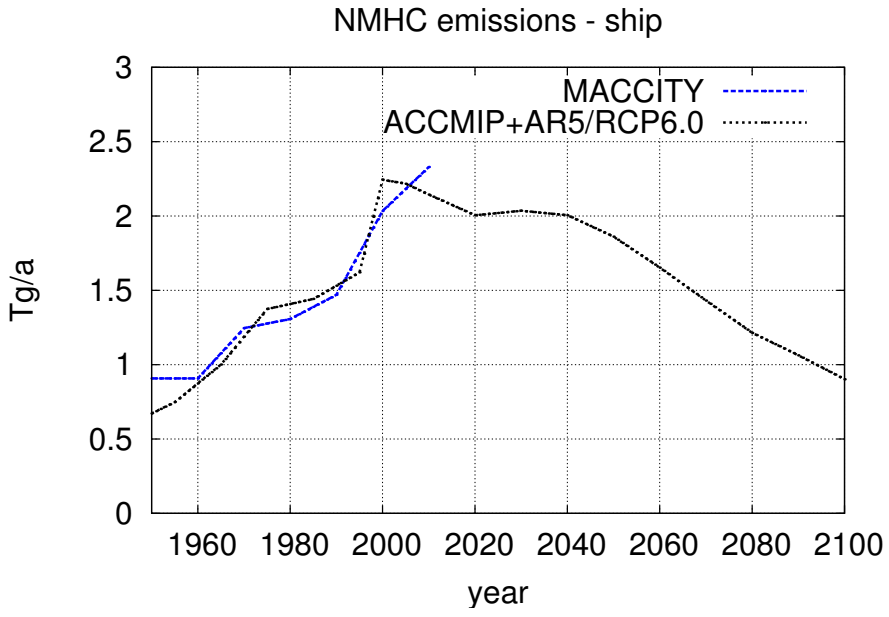

Figure E36: As Figure E33, but for NMHC (in Tg(C)/a).

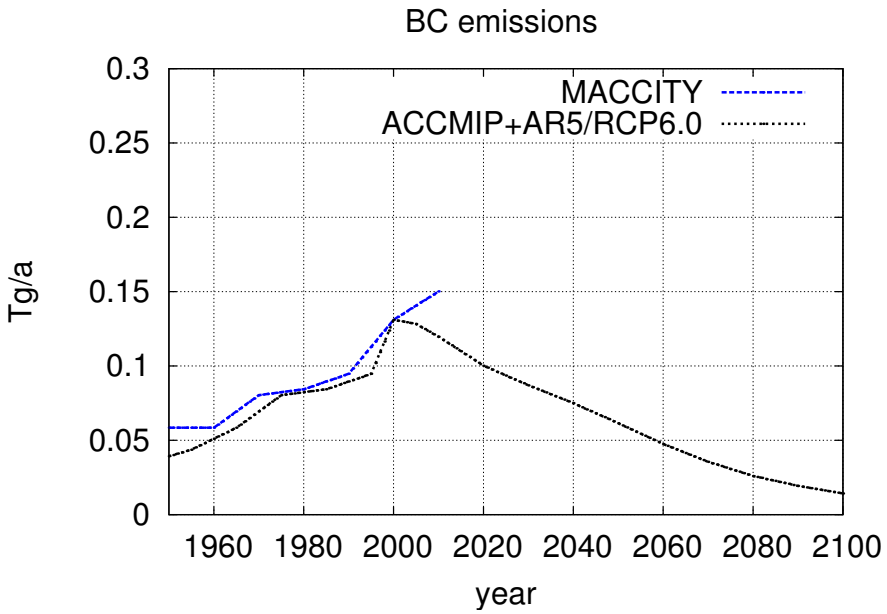

Figure E37: As Figure E33, but for black carbon (in Tg(C)/a).

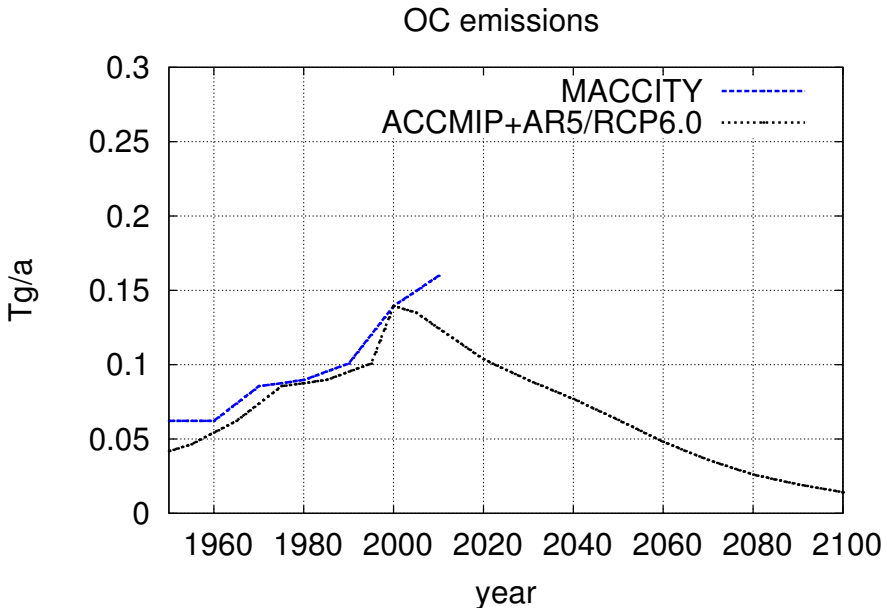

Figure E38: As Figure E33, but for organic carbon (in Tg(C)/a).

4.3.5 Aviation

From the aviation (aircraft) sector, only NOx is emitted in the *-base-* and *-oce-* simulations, in *-aero-* and *-aecl-* black carbon (BC) in addition. The totals for the different years are shown in Figures E39 and E40

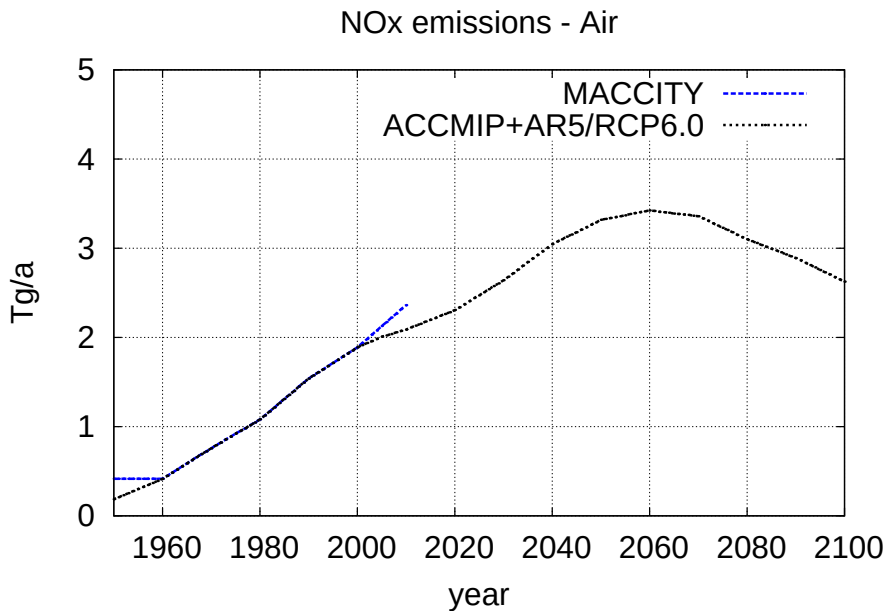

Figure E39: Annual total emissions of NOx from the aviation ("air"craft) sector (in Tg(NO)/a).

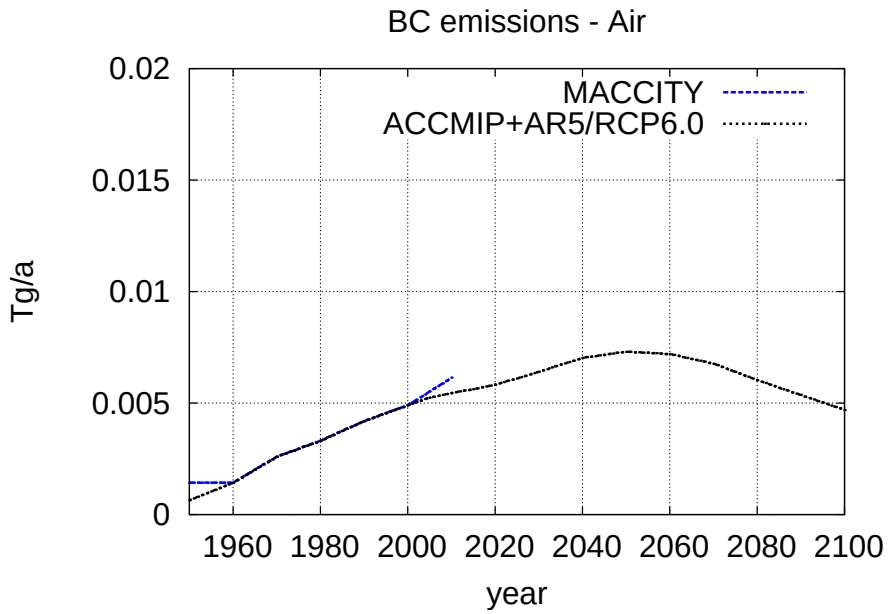

Figure E40: Annual total emissions of BC from the aviation ("air"craft) sector (in Tg(C)/a).

4.3.6 Land without road and awb

Figures E41 - E47 show the annual total emissions from all anthropogenic land sources without road- and awb-emissions. MACCity and ACCMIP+AR5/RCP6.0 are identical between 1960 and 2000, except for NMHC and organic carbon. Starting 2000, the MACCity data follows the RCP8.5 scenario, while the ACCMIP+AR5/RCP6.0 follows the RCP 6.0 scenario.

Compared to the other sectors, there is one important difference for the NMHC from this sector: The MACCity total NMHC emissions are larger than those of ACCMIP+AR5/RCP6.0, up to ∼15 Tg(C)/a. The difference between both estimates is not constant over time.

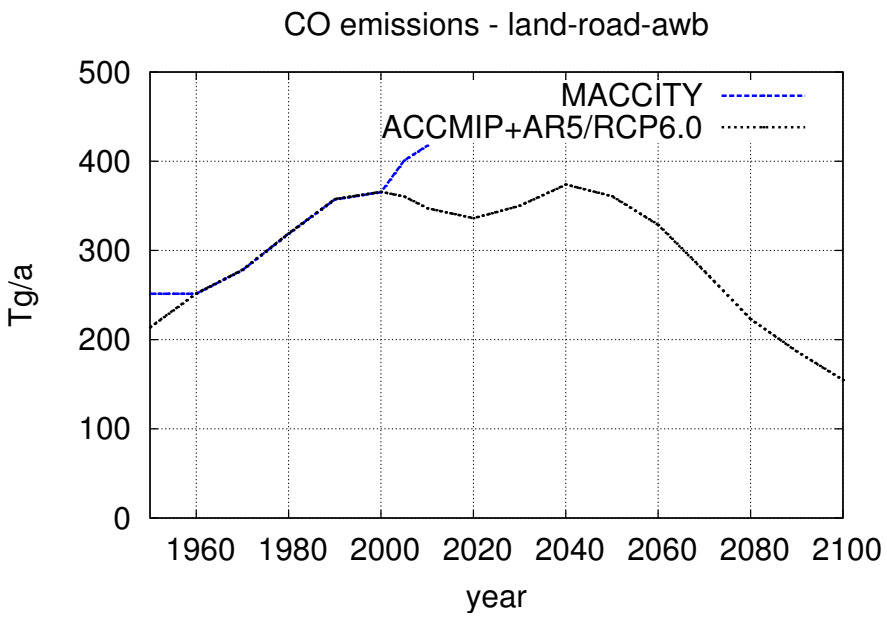

Figure E41: Annual total emissions of CO from the land sector (without road and awb).

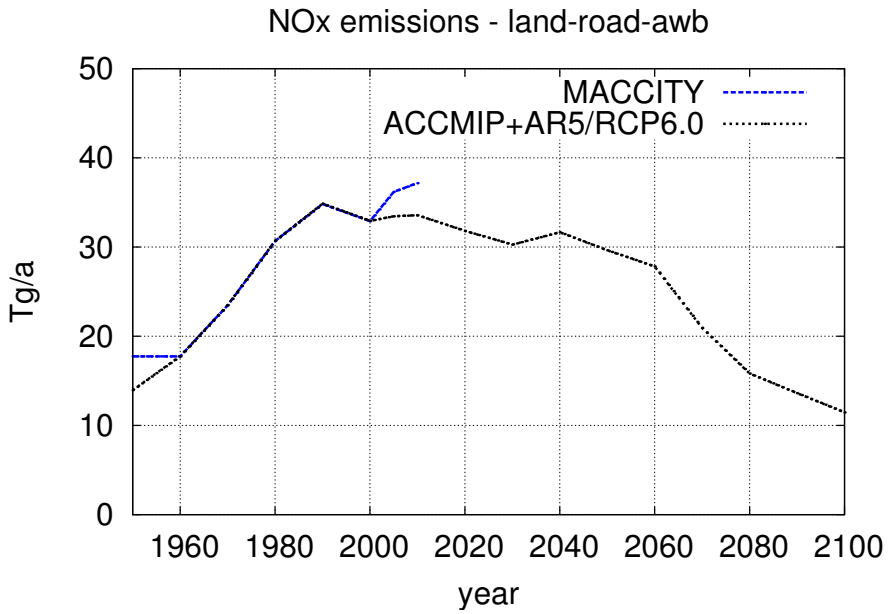

Figure E42: As Figure E41, but for NOx (in Tg(NO)/a).

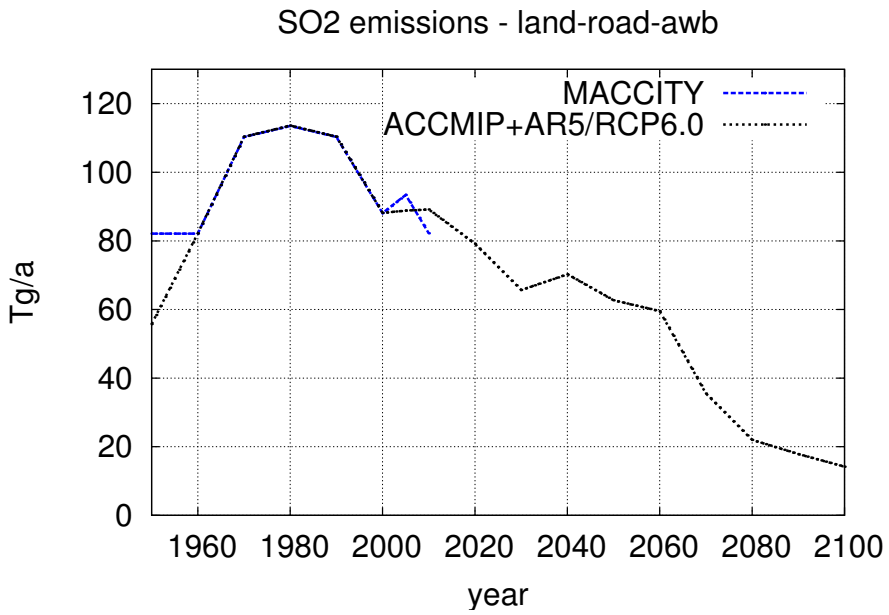

Figure E43: As Figure E41, but for SO_2.

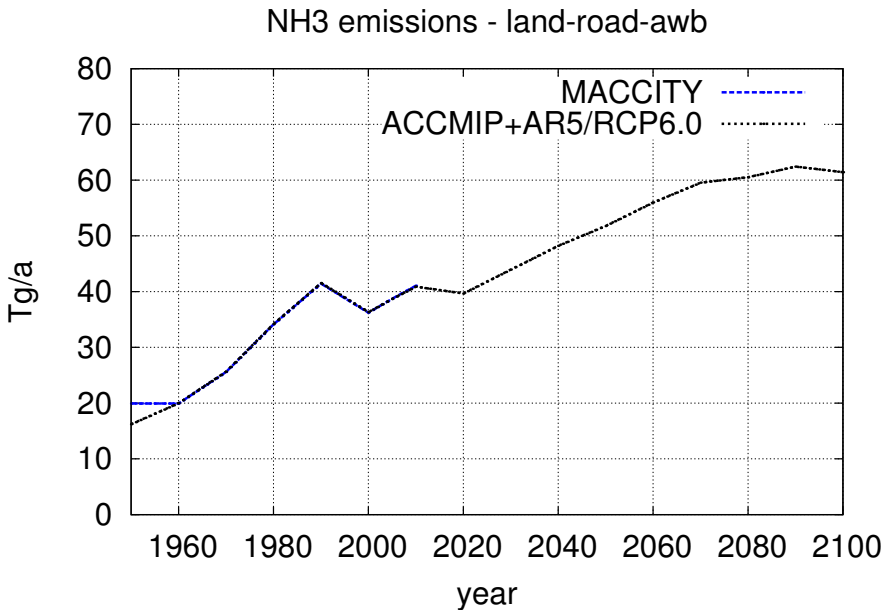

Figure E44: As Figure E41, but for NH_3.

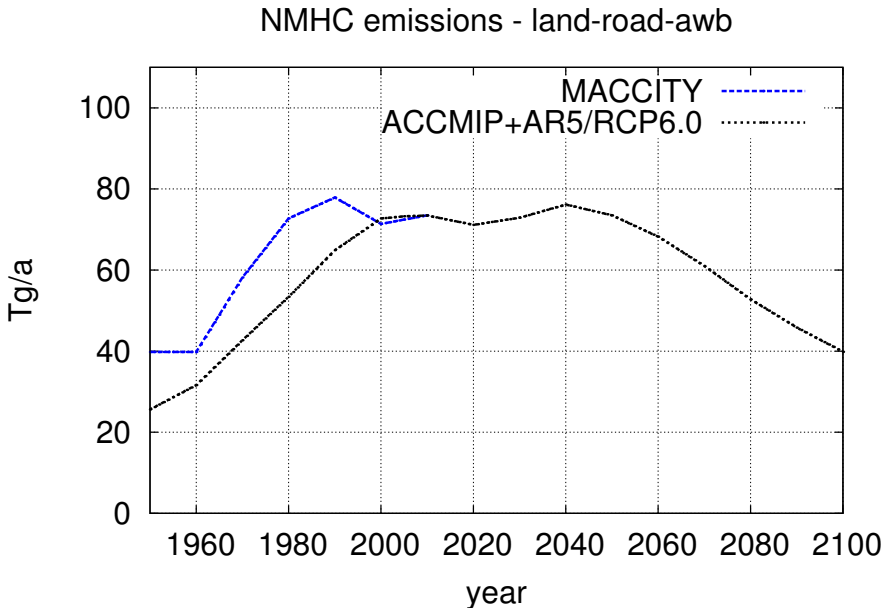

Figure E45: As Figure E41, but for total NMHC (in Tg(C)/a).

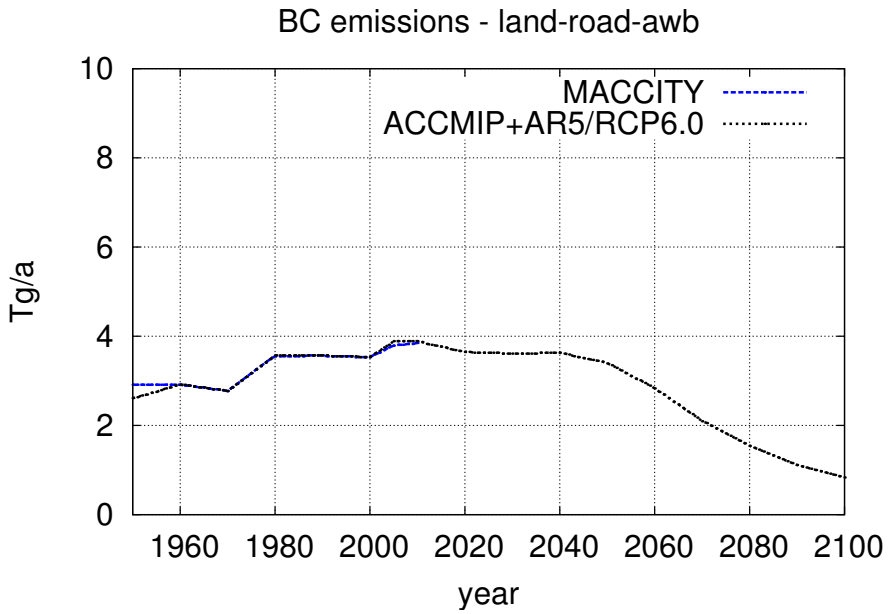

Figure E46: As Figure E41, but for total black carbon (in Tg(C)/a).

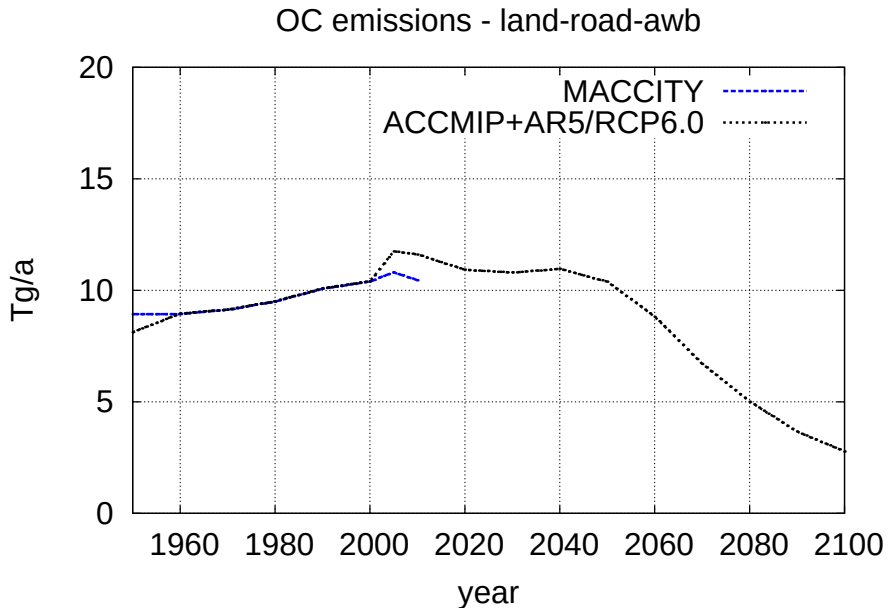

Figure E47: As Figure E41, but for total organic carbon (in Tg(C)/a).

4.3.7 Anthropogenic emissions without emissions from aviation

Figures E48 - E54 show the anthropogenic annual total emissions without emissions from aircraft. For CO, NOx, SO_2, NH_3, black and organic carbon the typical time evolution of the emissions is apparent. The small differences between the MACCity and the ACCMIP+RCP6.0 estimates arise mostly from the different reference times applied to the ship emissions in both data sets. Despite the fact that the NH_3 emissions of the RCP6 and RCP8.5 differ for the awb and the road sector, the annual total emissions for both data sets are identical from 1960 on (see Figure E51). While the NMHC emissions differ in the individual sectors by up to 200% between the MACCity and the ACCMIP+AR5/RCP6.0 inventories, the total emissions of the MACCity dataset are about 10% larger. This is well within the range of expected uncertainties.

In addition to the total emissions of the MACCity and the ACCMIP+AR5/RCP6.0 inventories, the total emissions of all simulations with the wrong timing for the road traffic sector (for details see description of the road traffic sector above) are shown in red (MACCity) and green (ACCMIP+AR5/RCP6.0). For NH_3 and SO_2 this mistake has only a minor influence on the total emissions, because the road traffic sector is only of minor importance as source for these species. For CO, NOx and the NMHC, the effectively resulting emission totals are underestimating the intended emissions, at least before the year 2080. After this year, the situation is vice versa, i.e., the effective (erroneous) emissions are larger than the intended.

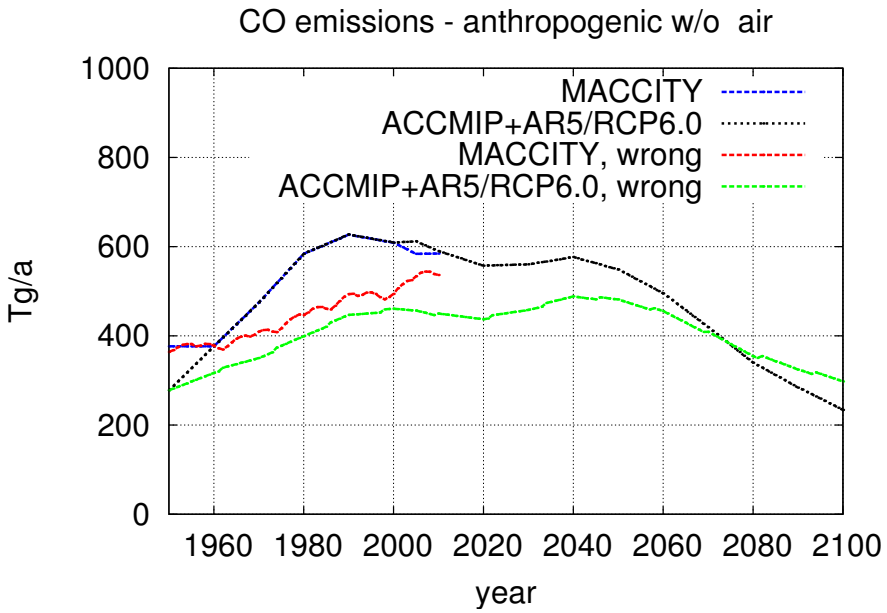

Figure E48: Annual total emissions of CO from all anthropogenic emission sectors, except for aviation. The totals marked as "wrong" indicate the effectively used totals for the simulations with the wrong timing of the road traffic sector.

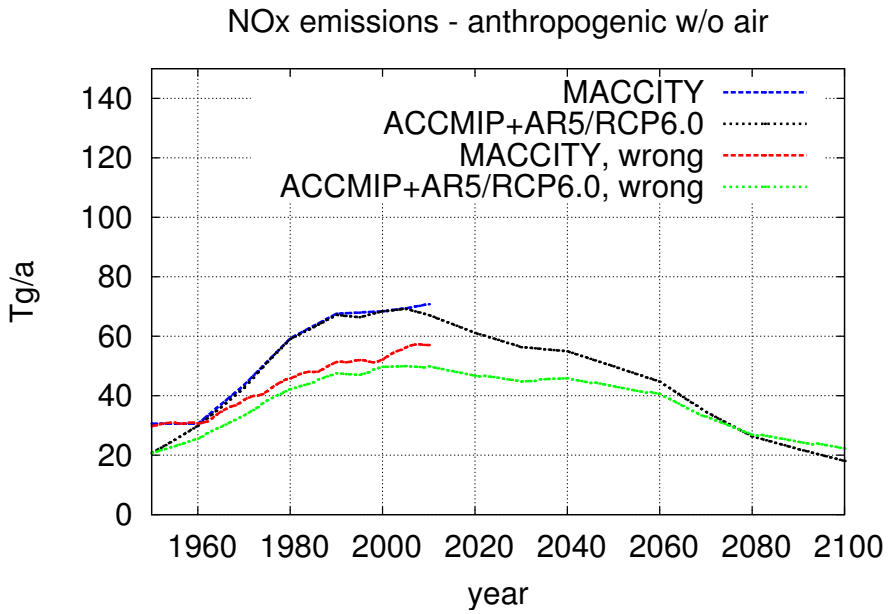

Figure E49: As Figure E48, but for NOx (in Tg(NO)/a).

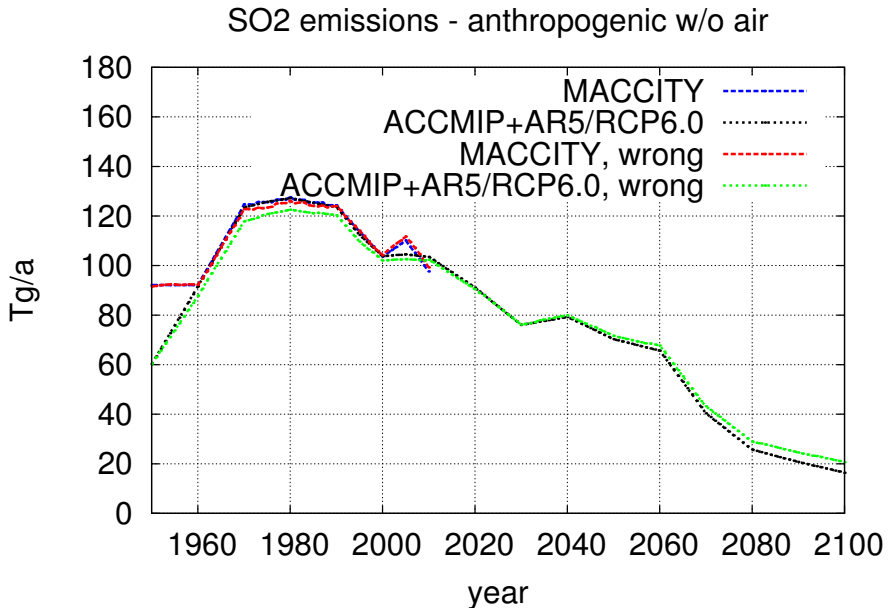

Figure E50: As Figure E48, but for SO_2.

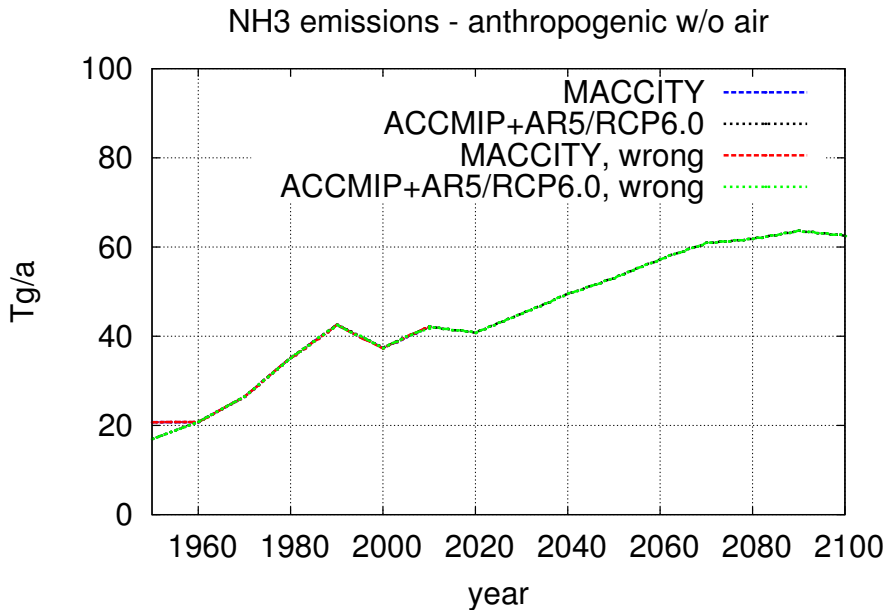

Figure E51: As Figure E48, but for NH_3.

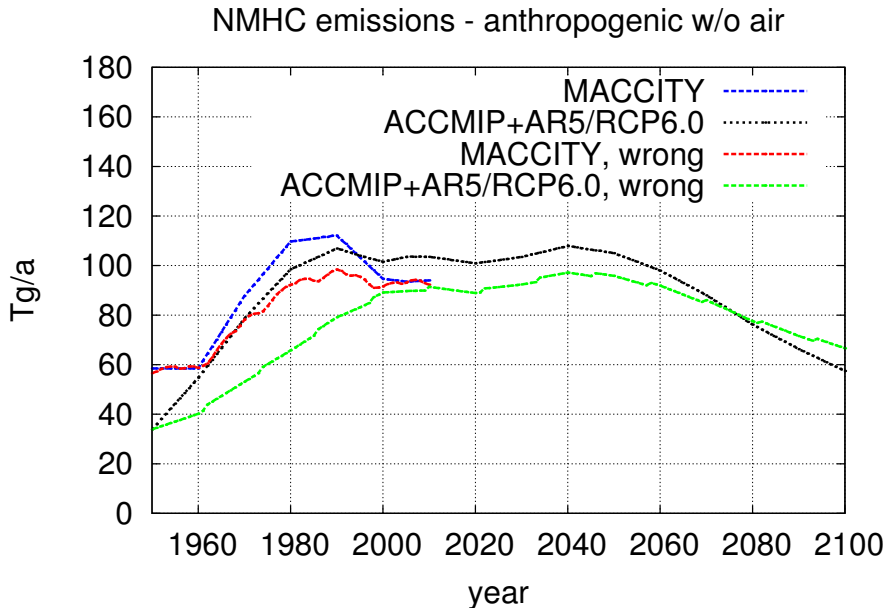

Figure E52: As Figure E48, but for total NMHC (in Tg(C)/a).

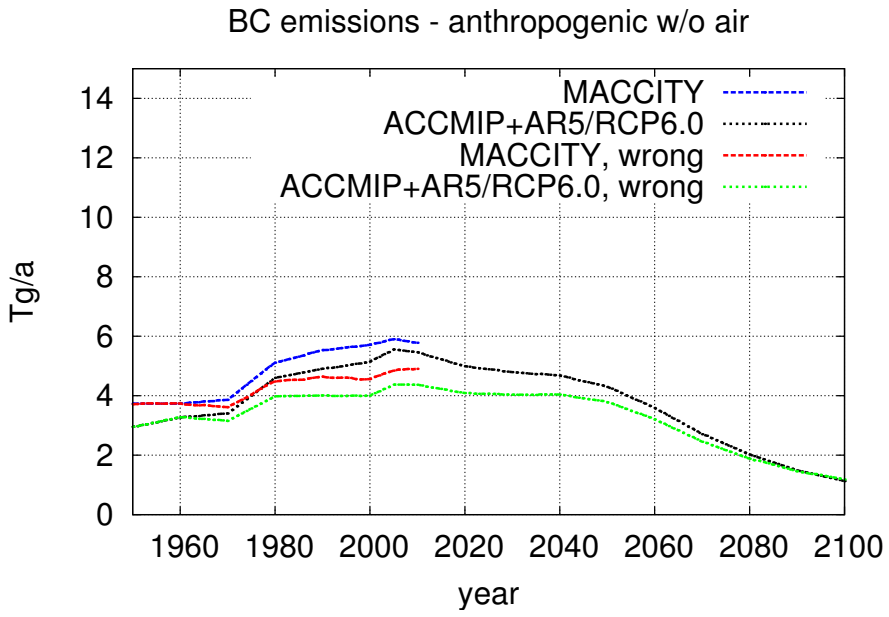

Figure E53: As Figure E48, but for total black carbon (in Tg(C)/a).

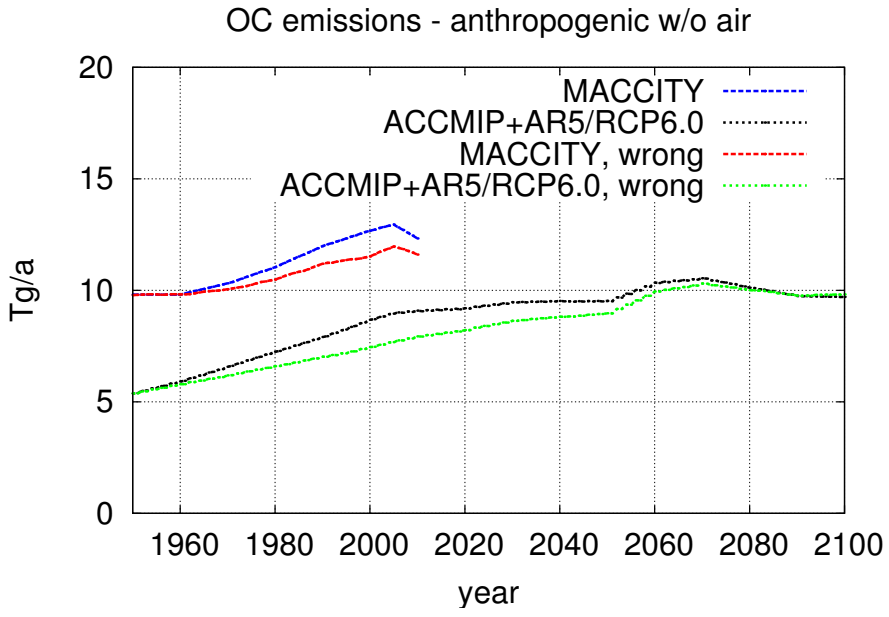

Figure E54: As Figure E48, but for total organic carbon (in Tg(C)/a).

4.4 Remarks

Comparing both inventories of anthropogenic emissions a few remarks are highlighted:

- The total emissions from the different sectors of CO, NOx, SO_2 and NH_3 are identical between MACCity and ACCMIP+AR5/RCP6.0, but
- the reference time of the decadal ship emission estimates are shifted by five years. This has no significant impact on the annual total emissions, but must be kept in mind when comparing the impact of ship emissions.
- The anthropogenic total NMHC emissions of both inventories are qualitatively very similar, differing by about 10%. While this is within the range of expected uncertainties, significant differences are apparent for the individual sectors. This implies also differences in the geographical distribution of emissions.

4.5 Emissions of diagnostic tracers

As listed in the Appendix A5 and Table A1 of the manuscript, additional diagnostic tracers have been included in the model simulations. One, SF6_CCMI has been directly emitted. The time series (annual values) is shown in Figure E55.

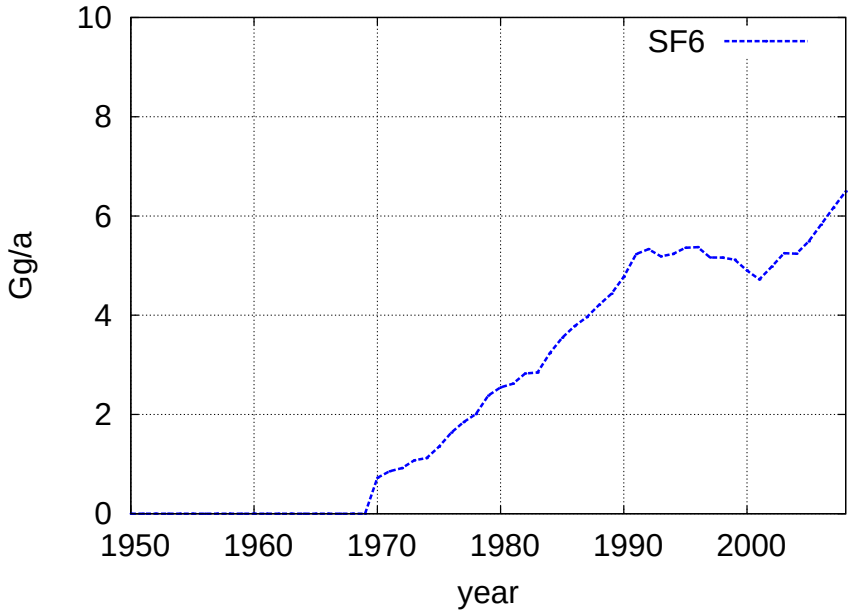

Figure E55: Emissions of SF6_CCMI (in $Gg(SF_6)/a$) according to the EDGAR (v4.2) database. The corresponding data file is EDGAR_v42DLR1.0_IPCC_anth_SF6_1950-2008.nc. From year 2009 on, data of the year 2008 has been repeated.

The corresponding data files used for the diagnostic tracers are listed in Table E1.

Tracer	Data file
SF6	CCMI_DLR1.0_RCP6.0_sfmr_SF6_195001-210012.nc
AOA	DLR_1.0_X_sfmr_AOA_195001-210012.nc
SF6_AOA	FUB_1.1_X_sfmr_AOA_195001-210012.nc
SF6_AOAc	FUB_1.1_X_sfmr_AOAc_195001-210012.nc
SF6_CCMI	EDGAR_v42DLR1.0_IPCC_anth_SF6_1950-2008.nc
SO_2t	(see Table A1 in manuscript)
NH_05	CCMI_DLR1.0_X_X_synth_const.nc (NH)
NH_50	CCMI_DLR1.0_X_X_synth_const.nc (NH)
NH50W	CCMI_DLR1.0_X_X_synth_const.nc (NH)
AOA_NH	CCMI_DLR1.0_X_X_synth_const.nc (ZERO)
ST80_25	CCMI_DLR1.0_X_X_synth_const.nc (ST80)
CO_25	(see Table A1 in manuscript)
CO_50	(see Table A1 in manuscript)
AOA_CCMI	CCMI_DLR1.0_X_X_synth_const.nc (ZERO)
O_3(s)	(see Table A1 in manuscript)

Table E1: Data files used for the different diagnostic tracers, see Table A1 in manuscript. Names in parentheses denote the variable names.

5 Non-anthropogenic emissions

In addition to the prescribed anthropogenic emissions, emissions from natural sources have been prescribed as well, either as monthly resolved or annually constant climatology (cyclically repeated for all simulated years).

The Non-Methane Hydrocarbons (NMHCs) are based on the spatial and temporal distribution of the GEIA (Global Emissions InitiAtive)[4] NMHCs distribution as described by Guenther et al. (1995). The distributions are available for isoprene, terpenes and other volatile organic compounds, which were then scaled to the total global annual emissions according to recent literature (see Table E3).

Table E2 shows the input files that were used to account for these additional off-line emissions.

Input files with non-anthropogenic emissions	
Group	Input file(s)
Biogenic Emissions	GEIA_MPIC1.0_X_bio_MISC_200001_200012.nc
Ammonia	GEIA_MPIC1.0_X_bioland_NH3_2000-2000.nc
	GEIA_MPIC1.0_X_biowater_NH3_2000-2000.nc
Terrestrial DMS	SpiroKettle_MPIM1.0_clim_bio_DMS_01-12.nc
Halocarbons	Warwick_UMZ1.0_clim_biowater_BrCarbons_X-X.nc
Methyl Iodide	Bell_2002_X_all_CH3I_20001-200012.nc
Volcanic SO_2 (*-base-*)	AEROCOM_DLR1.0_X_volc_SO2_200001-200012.nc
Volcanic SO_2 (*-aero-, -aecl-*)	AEROCOM-DIEHL_UMZ1.0_X_X_volc_SO2_195001_201012.nc
OC from SOA (*-aero-, -aecl-*)	AEROCOM_UMZ1.0_X_SOA_OC_200001-200012.nc

Table E2: List of input files with additional non-anthropogenic emissions used for the ESCiMo simulations.

The annual emissions are displayed in Table E3 along with the respective references and the seasonal variation, if present. Apart from terrestrial DMS and OC, which are given in Tg(S)/a and Tg(C)/a, respectively, all other totals show Tg(species)/a. Emission data are specified as flux in molec/m^2/s, except for the volcanic SO_2 emissions, which are provided as a volume flux in molec/m^3/s on fixed pressure levels. Hence, although the flux is constant, the actual emitted mass of volcanic SO_2 depends slightly on the state of the model atmosphere (due to the pressure based vertical model grid) and therefore differs between the simulations. Here, we present a representative value for the emissions using standard atmosphere conditions.

The following list contains further explanations and references corresponding to the superscripts in Table E3:

1. Rudolph (1997) states that several Tg/a come from plants. Upon stress, plant emissions of C_2H_4 can increase drastically (Fall, 1999), therefore any global extrapolation of the emissions is highly uncertain. Here, we assumed 3 Tg/a from soil (Sawada and Tutsuka, 1986) and 7 Tg/a from vegetation (von Kuhlmann, 2001). An additional 1.4 Tg/a were added for the ocean, which is the upper limit proposed by Plass-Dülmer et al. (1995).

2. Kesselmeier and Staudt (1999) citing Guenther et al. (1994) claim a low contribution of terrestrial vegetation to the atmospheric budget, thus we set emissions from land to zero. The oceanic contribution was estimated to be 0.54 Tg/a (upper limit of Plass-Dülmer et al., 1995).

3. The contribution to propene (C_3H_6) by sources over land is estimated to be 2.15 Tg/a. This value is based on a molecule emission ratio of ethene to propene of 2.63/1.13 (measurements in forest by Goldstein et al., 1996) and the assumption of a non-stress emission of $\sim$ 3.3 Tg/a for ethene. The oceanic contribution was estimated to be 1.27 Tg/a (upper limit of Plass-Dülmer et al., 1995).

4. Kesselmeier and Staudt (1999) citing Guenther et al. (1994) claim a low contribution of terrestrial vegetation to the atmospheric budget, thus we set emissions from land to zero. The oceanic contribution was estimated to be 0.35 Tg/a (upper limit of Plass-Dülmer et al., 1995).

5. The contribution from land was estimated to be 3.4 Tg/a based on the ranges of given in literature (e.g., 0.5-5.6 Tg/a Bode et al. (1997), 0.6-2.0 Tg/a Kesselmeier et al. (1998), 1.4 Tg/a from Savanna soils (Helas and Kesselmeier, 1993)).

[4] GEIAv1 database

Non-anthropogenic emissions			
Species	Reference	Seasonal range in Tg/a	Tg/a
Biogenic Emissions			
C_2H_4		9.58 - 14.08	11.36[1)]
C_2H_6		-	0.539[2)]
C_3H_6		3.01 - 4.00	3.41[3)]
C_3H_8		-	0.349[4)]
CH_3CO_2H		2.76 - 4.31	3.387[5)]
CH_3COCH_3	Folberth et al. (2006)	44.68 - 72.89	55.73
CH_3OH	Jacob et al. (2005)	122.6 - 191.6	150.46
CO		92.9 - 143.3	112.61[6)]
HCOOH		4.47 - 7.30	5.58[7)]
NC_4H_{10}		-	0.40[8)]
Ammonia			
NH_3(bioland)	Bouwman et al. (1997)[12)]	-	2.44
NH_3(biowater)	Bouwman et al. (1997)[12)]	-	8.16
Terrestrial DMS			
DMS (Tg(S)/a)	Spiro et al. (1992)	0.51 - 1.70	0.91
Halocarbons			
$CHBr_3$	Warwick et al. (2006)	-	0.595
CH_2BrCl	Warwick et al. (2006)	-	0.0068
CH_2Br_2	Warwick et al. (2006)	-	0.113
$CHBr_2Cl$	Warwick et al. (2006)	-	0.023
$CHBrCl_2$	Warwick et al. (2006)	-	0.016
Methyl Iodide			
CH_3I	Bell et al. (2002)	0.185 - 0.25	0.213
Volcanic SO_2			
SO_2		-	30.43[9)]
SO_2		-	(see Figure E56)[10)]
Organic carbon (OC) from secondary organic aerosol (SOA)			
OC	Dentener et al. (2006)	13.62 - 27.20	19.14[11)]

Table E3: Summary of totals of applied off-line emissions. If a seasonal cycle is present in the data, its range is given in the third column. Superscripts refer to the text passage below with further explanations.

6. The contribution from land was estimated to 100 Tg/a. This estimate comprises CO from the oxidation of some (non-industrial) hydrocarbons, which are not being accounted for by other emissions, i.e. higher alkenes (C>3), terpene products other than acetone, as well as higher aldehydes etc.. Additionally, direct CO emissions from vegetation and plant decay are accounted for by this estimate. For the oceanic contribution, we used the estimate of 13 Tg/a from Bates et al. (1995).

7. The contribution from land was estimated to be 5.6 Tg/a, based on the literature with estimates ranging from 0.6 to 11.0 Tg/a (e.g., 0.6-11.0 Tg/a (Bode et al., 1997), 0.9-6.0 Tg/a (Kesselmeier et al., 1998), 1.6 Tg/a from Savanna soils (Helas and Kesselmeier, 1993)).

8. The oceanic contribution was estimated to be 0.4 Tg/a, based on the estimate of 0.11 Tg/a of butanes by Plass-Dülmer et al. (1995), which was upscaled to 0.19 Tg/a (upper limit of the same study) to account for other alkanes. Note that all C_4H_{10} emissions (including those accounting for other alkenes), have been emitted into the NC_4H_{10} tracer.

9. For the *-base-* simulations, we used monthly resolved volcanic SO_2 emissions of the year 2000, including both explosive and continuously degassing volcanoes. Both are taken from AEROCOM (Dentener et al., 2006). The emissions are linearly distributed in an altitude range around the volcano top, using different ranges for explosive and continuously-degassing volcanoes. Volcano altitudes are taken from the study by Halmer et al. (2002).

10. For the *-aero-* and *-aecl-* simulations, we used a monthly resolved time series. It comprises the emissions from continuously degassing volcanoes (AEROCOM, Dentener et al., 2006, based on the GEIA inventory (Andres and

Kasgnoc, 1998)) and those of eruptive volcanoes based on AEROCOM[5]. Figure E56 shows the time series.

11. The emissions from the file are scaled by a factor of 1.4 to account for the organic carbon (OC) representing particulate organic matter (POM, Seinfeld and Pandis, 1997; Ferek et al., 1998). The resulting carbon emissions are distributed into the hydrophilic (65%) and hydrophobic (35%) Aitken modes of OC. This has been used in the *-aero-* and *-aecl-* simulations, only.

12. downloaded from `http://themasites.pbl.nl/tridion/en/themasites/geia/index.html`

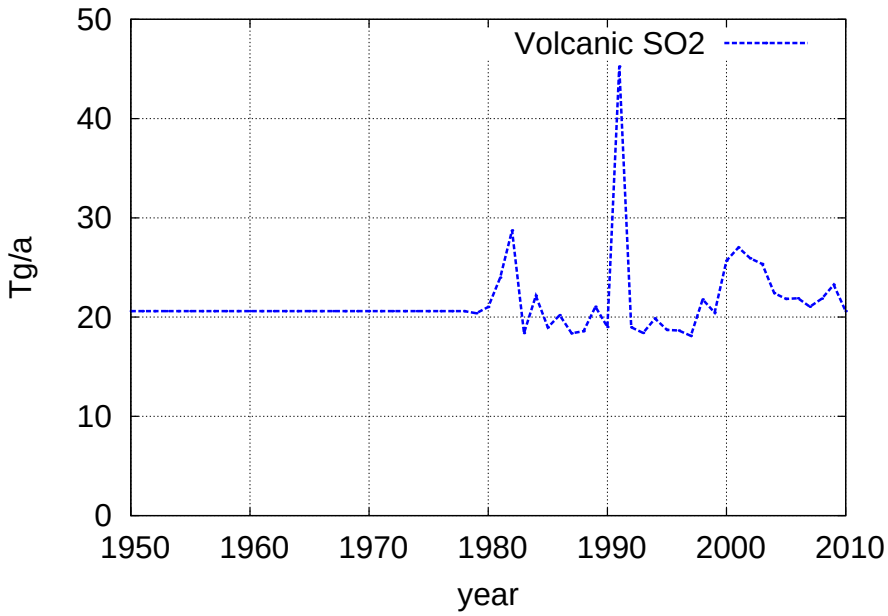

Figure E56: Emissions of SO_2 (in $Tg(SO_2)/a$) from volcanic activity (continuously degassing and eruptive) as prescribed in the *-aero-* and *-aecl-* simulations.

6 Boundary conditions for on-line calculated emissions

[5] `http://wiki.seas.harvard.edu/geos-chem/index.php/Volcanic_SO2_emissions_from_Aerocom`

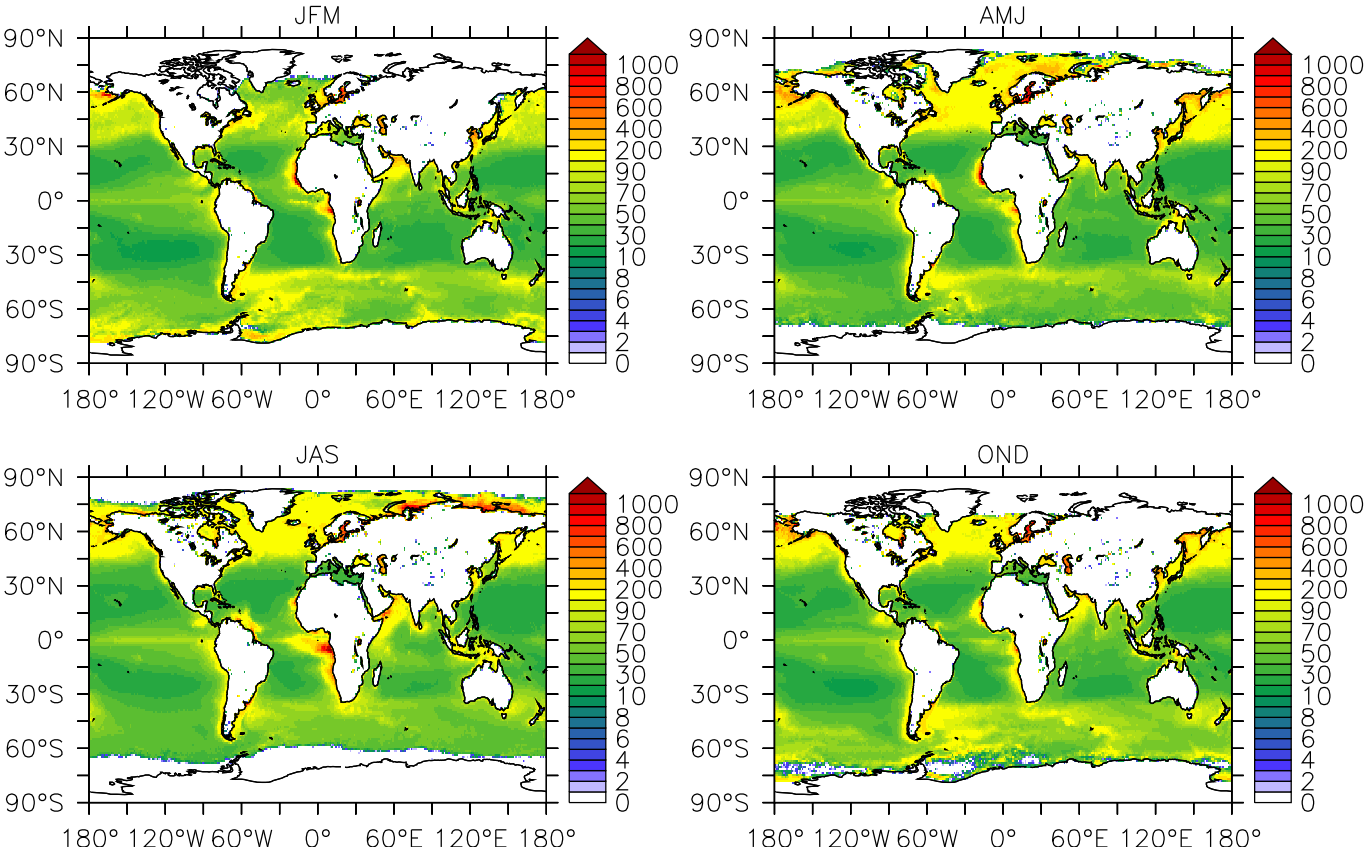

Figure E57: Climatological seasonal particulate organic carbon (POC, in $\mathrm{mg\,m^{-3}}$) in ocean surface water derived from SEAWIFS-Aqua (summer 2002 – summer 2010). This input data is used to calculate the POC emission from the sea-salt emissions (in submodel ONEMIS) and has been used in the *-aero-* and *-aecl-* simulations. The corresponding data file is seawifs_1.0_seasonal_X_POC_01-04.nc.

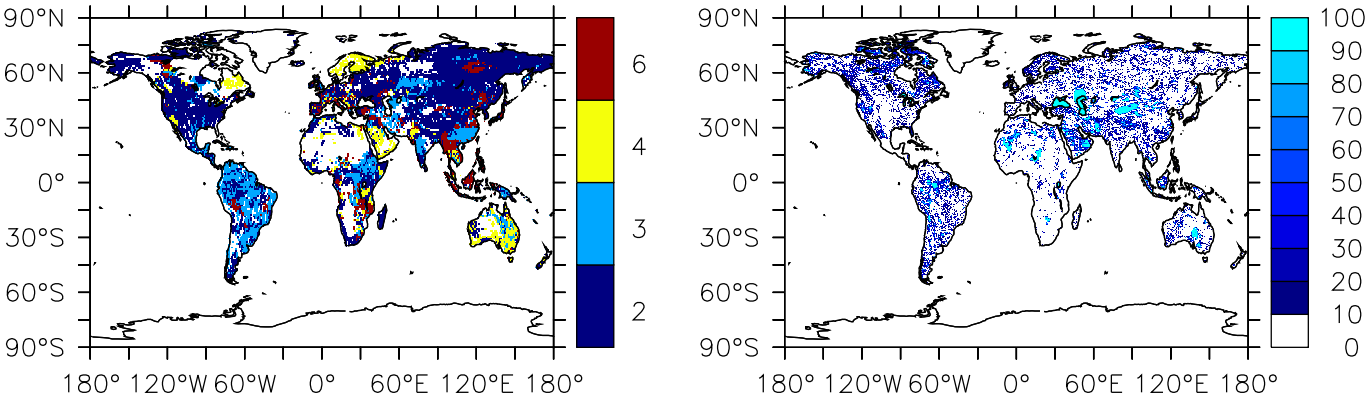

Figure E58: Soil type index (left) and areal coverage of preferential dust sources, expressed as percentage of each 0.5^o x 0.5^o grid cell (right), according to Tegen et al. (2002). The corresponding data files are Tegen_1.0_X_soilType_X-X.nc and Tegen_1.0_X_potSource_X-X.nc, respectively.

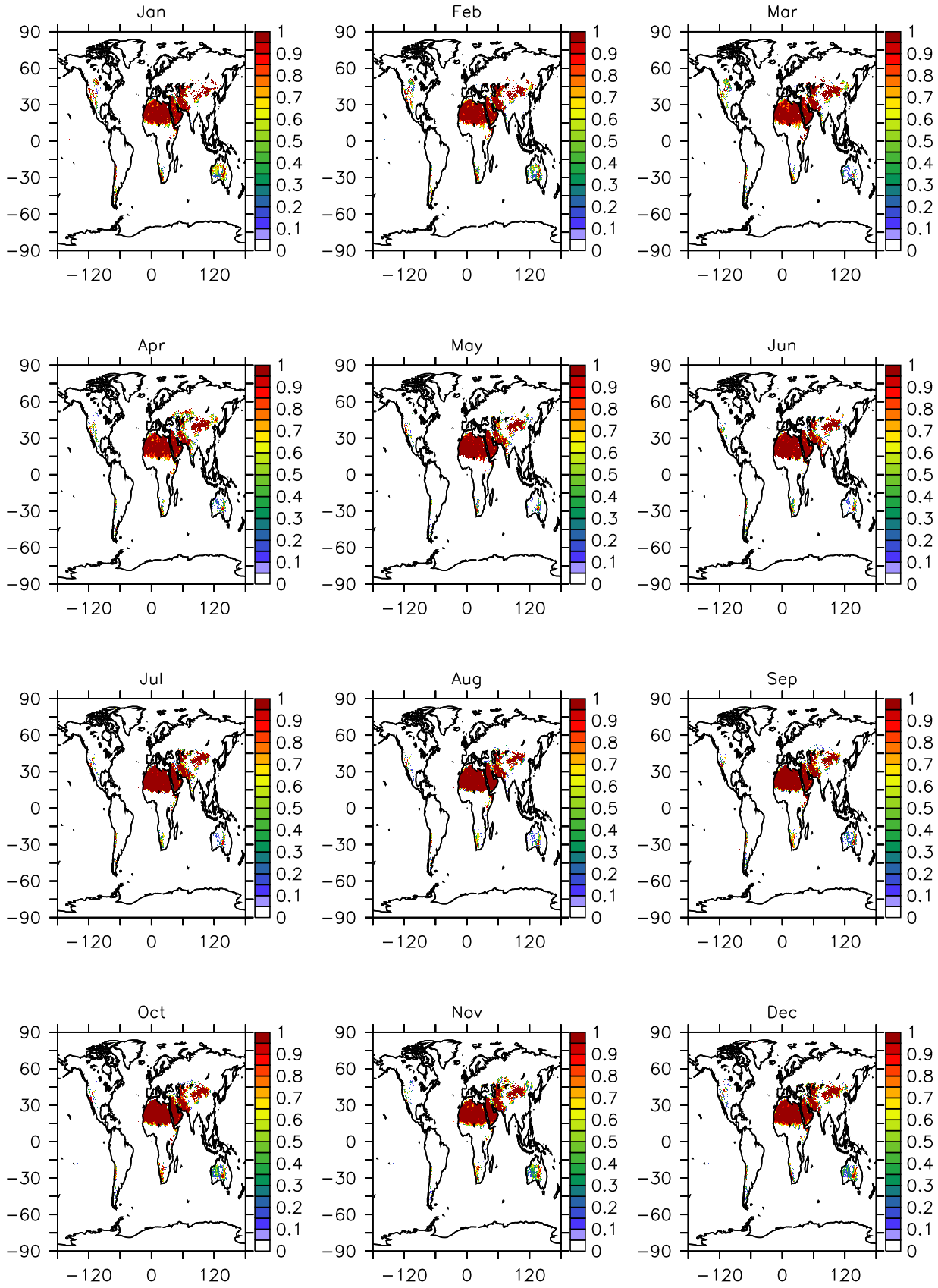

Figure E59: Seasonal cycle of surface area fraction not covered by vegetation, i.e., where dust can be emitted. The corresponding data file is Tegen_1.0_X_ndviLAIeff_01-12.nc.

Submodel	Input file(s)
MECCA_KHET	Righi_DLR1.0_clim_X_MADEAerosolSurface_01-12.nc
AIRSEA	WOA_MPIC1.0_clim_ocean_salinity_01-12.nc (salt)
	SOLAS_1.0_X_seaconc_DMS_200001_200012.nc (DMS_SEA)
	WOA_MPIC1.0_clim_C5H8_200001-200012.nc (C5H8_w)
ONEMIS	X_X_X_surfpara_X_01-12.nc
	X_X_X_X_VOC_X-X.nc
	X_X_X_X_NO_X-X.nc
	X_X_X_X_NOemisclass1_X-X.nc
	X_X_X_X_NOemisclass2_X-X.nc
DDEP	X_X_X_soilpHcl_X_X-X.nc
	X_X_X_surfpara_X_01-12.nc
AEROPT	CCMI-ETH_MPIC1.1_hist_optLW-ECHAM5_X_195001-201112.nc
	CCMI-ETH_MPIC1.1_hist_optSW-ECHAM5_X_195001-201112.nc
	aeropt_lw_1.59_1.59_2.00.nc*
MSBM	CCMI-ETH_MPIC1.1_hist_X_H2SO4_195001-201112.nc
JVAL	HALOE_MPIC1.0_clim_X_O3_01-12.nc*
	(*RC1*) NRLSSI_FUB1.0_hist_X_solar1AU_19500101_20111231.txt (solact)
	(*RC2*) NRLSSI_FUB1.0_HadGEM_X_solar1AU_19500101_21001231.txt (solact)
RAD_FUBRD	(*RC1*) NRLSSI_FUB1.0_hist_X_spec055_19500101_20111231.txt
	(*RC2*) NRLSSI_FUB1.0_HadGEM_X_spec055_19500101_21001231.txt

Table E4: Additional data files (here not visualised) used as input for the indicated submodels. Names in parentheses denote the variable names. The asterisk indicates files which are directly imported by the submodel, and not by IMPORT.

References

Andres, R. J. and Kasgnoc, A. D.: A time-averaged inventory of subaerial volcanic sulfur emissions, Journal of Geophysical Research: Atmospheres, 103, 25 251–25 261, doi:10.1029/98JD02091, URL http://dx.doi.org/10.1029/98JD02091, 1998.

Bates, T. S., Kelly, K. C., Johnson, J. E., and Gammon, R. H.: Regional and seasonal variations in the flux of oceanic carbon monoxide to the atmosphere, J. Geophys. Res., 100, 23 093–23 101, 1995.

Bell, N., Hsu, L., Jacob, D. J., Schultz, M. G., Blake, D. R., Butler, J. H., King, D. B., Lobert, J. M., and Maier-Reimer, E.: Methyl iodide: Atmospheric budget and use as a tracer of marine convection in global models, Journal of Geophysical Research: Atmospheres, 107, ACH 8–1–ACH 8–12, doi:10.1029/2001JD001151, URL http://dx.doi.org/10.1029/2001JD001151, 4340, 2002.

Bode, K., Helas, G., and Kesselmeier, J.: Biogenic contribution to atmospheric organic acids, in: Biogenic Volatile Organic Compounds in the Atmosphere - Summary of Present Knowledge, edited by Helas, G., Slanina, S., and Steinbrecher, R., pp. 157–170, SPB Academic Publishers, Amsterdam, The Netherlands, 1997.

Bouwman, A. F., Lee, D. S., Asman, W. A. H., Dentener, F. J., Van Der Hoek, K. W., and Olivier, J. G. J.: A global high-resolution emission inventory for ammonia, Global Biogeochemical Cycles, 11, 561–587, doi:10.1029/97GB02266, URL http://dx.doi.org/10.1029/97GB02266, 1997.

Brühl, C., Lelieveld, J., Crutzen, P. J., and Tost, H.: The role of carbonyl sulphide as a source of stratospheric sulphate aerosol and its impact on climate, Atmospheric Chemistry and Physics, 12, 1239–1253, doi:10.5194/acp-12-1239-2012, URL http://www.atmos-chem-phys.net/12/1239/2012/, 2012.

Dentener, F., Kinne, S., Bond, T., Boucher, O., Cofala, J., Generoso, S., Ginoux, P., Gong, S., Hoelzemann, J. J., Ito, A., Marelli, L., Penner, J. E., Putaud, J.-P., Textor, C., Schulz, M., van der Werf, G. R., and Wilson, J.: Emissions of primary aerosol and precursor gases in the years 2000 and 1750 prescribed data-sets for AeroCom, Atmospheric Chemistry and Physics, 6, 4321–4344, doi:10.5194/acp-6-4321-2006, URL http://www.atmos-chem-phys.net/6/4321/2006/, 2006.

Fall, R.: Chapter 2 - Biogenic Emissions of Volatile Organic Compounds from Higher Plants, in: Reactive Hydrocarbons in the Atmosphere, edited by Hewitt, C. N., pp. 41 – 96, Academic Press, San Diego, doi:http://dx.doi.org/10.1016/B978-012346240-4/50003-5, URL http://www.sciencedirect.com/science/article/pii/B9780123462404500035, 1999.

Ferek, R. J., Reid, J. S., Hobbs, P. V., Blake, D. R., and Liousse, C.: Emission factors of hydrocarbons, halocarbons, trace gases and particles from biomass burning in Brazil, Journal of Geophysical Research: Atmospheres, 103, 32 107–32 118, doi:10.1029/98JD00692, URL http://dx.doi.org/10.1029/98JD00692, 1998.

Folberth, G. A., Hauglustaine, D. A., Lathière, J., and Brocheton, F.: Interactive chemistry in the Laboratoire de Météorologie Dynamique general circulation model: model description and impact analysis of biogenic hydrocarbons on tropospheric chemistry, Atmospheric Chemistry and Physics, 6, 2273–2319, doi:10.5194/acp-6-2273-2006, URL http://www.atmos-chem-phys.net/6/2273/2006/, 2006.

Goldstein, A. H., Fan, S. M., Goulden, M. L., Mungern, J. W., and Wofsy, S. C.: Emissions of ethene, propene, and I-butene by a midlatitude forest, J. Geophys. Res., 101, 9149–9157, 1996.

Granier, C., Bessagnet, B., Bond, T., D'Angiola, A., van der Gon, H. D., Frost, G., Heil, A., Kaiser, J., Kinne, S., Klimont, Z., Kloster, S., Lamarque, J.-F., Liousse, C., Masui, T., Meleux, F., Mieville, A., Ohara, T., Raut, J.-C., Riahi, K., Schultz, M., Smith, S., Thompson, A., Aardenne, J., Werf, G., and Vuuren, D.: Evolution of anthropogenic and biomass burning emissions of air pollutants at global and regional scales during the 1980 - 2010 period, Climatic Change, 109, 163–190, 2011.

Guenther, A., Zimmerman, P., and Wildermuth, M.: Natural volatile organic compound emission rate estimates for U.S. woodland landscapes, Atmospheric Environment, 28, 1197 – 1210, doi:http://dx.doi.org/10.1016/1352-2310(94)90297-6, URL http://www.sciencedirect.com/science/article/pii/1352231094902976, 1994.

Guenther, A., Hewitt, C. N., Erickson, D., Fall, R., Geron, C., Graedel, T., Harley, P., Klinger, L., Lerdau, M., Mckay, W. A., Pierce, T., Scholes, B., Steinbrecher, R., Tallamraju, R., Taylor, J., and Zimmerman, P.: A global model of natural volatile organic compound emissions, Journal of Geophysical Research: Atmospheres, 100, 8873–8892, doi:10.1029/94JD02950, URL http://dx.doi.org/10.1029/94JD02950, 1995.

Halmer, M., Schmincke, H.-U., and Graf, H.-F.: The annual volcanic gas input into the atmosphere, in particular into the stratosphere: a global data set for the past 100 years, Journal of Volcanology and Geothermal Research, 115, 511 – 528, doi:http://dx.doi.org/10.1016/S0377-0273(01)00318-3, URL http://www.sciencedirect.com/science/article/pii/S0377027301003183, 2002.

Helas, G. and Kesselmeier, J.: Estimates on sinks and sources of formic and acetic acid, in: General Assessment of Biogenic Emissions and Deposition of Nitrogen Compounds, Sulphur Compounds and Oxidants in Europe, edited by Slanina, J., Angeletti, G., and Beilke, S., pp. 299–304, CEC Air Pollution Research Report 47, E. Guyot SA, Brussels, 1993.

Hoor, P., Borken-Kleefeld, J., Caro, D., Dessens, O., Endresen, O., Gauss, M., Grewe, V., Hauglustaine, D., Isaksen, I. S. A., Jöckel, P., Lelieveld, J., Myhre, G., Meijer, E., Olivie, D., Prather, M., Schnadt Poberaj, C., Shine, K. P., Staehelin, J., Tang, Q., van Aardenne, J., van Velthoven, P., and Sausen, R.: The impact of traffic emissions on atmospheric ozone and OH: results from QUANTIFY, Atmospheric Chemistry and Physics, 9, 3113–3136, doi:10.5194/acp-9-3113-2009, URL http://www.atmos-chem-phys.net/9/3113/2009/, 2009.

IPCC: Atmospheric Chemistry and Greenhouse Gases, book section 4, pp. 240–288, Cambridge University Press, Cambridge, United Kingdom and New York, NY, USA, URL http://www.ipcc.ch/ipccreports/tar/wg1/, 2001.

Jacob, D. J., Field, B. D., Li, Q., Blake, D. R., de Gouw, J., Warneke, C., Hansel, A., Wisthaler, A., Singh, H. B., and Guenther, A.: Global budget of methanol: Constraints from atmospheric observations, Journal of Geophysical Research: Atmospheres, 110, D08 303, doi:10.1029/2004JD005172, URL http://dx.doi.org/10.1029/2004JD005172, 2005.

Kerkweg, A., Sander, R., Tost, H., and Jöckel, P.: Technical note: Implementation of prescribed (OFFLEM), calculated (ONLEM), and pseudo-emissions (TNUDGE) of chemical species in the Modular Earth Submodel System (MESSy), Atmospheric Chemistry and Physics, 6, 3603–3609, doi:10.5194/acp-6-3603-2006, URL http://www.atmos-chem-phys.net/6/3603/2006/, 2006.

Kesselmeier, J. and Staudt, M.: Biogenic Volatile Organic Compounds (VOC): An Overview on Emission, Physiology and Ecology, Journal of Atmospheric Chemistry, 33, 23–88, doi:10.1023/A:1006127516791, URL http://dx.doi.org/10.1023/A%3A1006127516791, 1999.

Kesselmeier, J., Bode, K., Gerlach, C., and Jork, E.-M.: Exchange of atmospheric formic and acetic acids with trees and crop plants under controlled chamber and purified air conditions, Atmospheric Environment, 32, 1765 – 1775, doi:10.1016/S1352-2310(97)00465-2, URL http://www.sciencedirect.com/science/article/pii/S1352231097004652, 1998.

Lamarque, J.-F., Bond, T. C., Eyring, V., Granier, C., Heil, A., Klimont, Z., Lee, D., Liousse, C., Mieville, A., Owen, B., Schultz, M. G., Shindell, D., Smith, S. J., Stehfest, E., Van Aardenne, J., Cooper, O. R., Kainuma, M., Mahowald, N., McConnell, J. R., Naik, V., Riahi, K., and van Vuuren, D. P.: Historical (1850 - 2000) gridded anthropogenic and biomass burning emissions of reactive gases and aerosols: methodology and application, Atmospheric Chemistry and Physics, 10, 7017–7039, doi:10.5194/acp-10-7017-2010, URL http://www.atmos-chem-phys.net/10/7017/2010/, 2010.

Plass-Dülmer, C., Koppmann, R., Ratte, M., and Rudolph, J.: Light nonmethane hydrocarbons in seawater, Global Biogeochemical Cycles, 9, 79–100, doi:10.1029/94GB02416, URL http://dx.doi.org/10.1029/94GB02416, 1995.

Pozzer, A., Jöckel, P., and Van Aardenne, J.: The influence of the vertical distribution of emissions on tropospheric chemistry, Atmospheric Chemistry and Physics, 9, 9417–9432, doi:10.5194/acp-9-9417-2009, URL http://www.atmos-chem-phys.net/9/9417/2009/, 2009.

Rudolph, J.: Biogenic sources of atmospheric alkenes and acetylene, in: Biogenic Volatile Organic Compounds in the Atmosphere - Summary of Present Knowledge, edited by Helas, G., Slanina, S., and Steinbrecher, R., pp. 53–65, SPB Academic Publishers, Amsterdam, The Netherlands, 1997.

Sawada, S. and Tutsuka, T.: Natural and anthropogenic sources of atmopsheric ethylene, 20, 821–832, 1986.

Schultz, M., Backman, L., Balkanski, Y., Bjoerndalsaeter, S., Brand, R., Burrows, J., Dalsøren, S., de Vasconcelos, M., Grodtmann, B., Hauglustaine, D., Heil, A., Hoelzemann, J., Isaksen, I., Kaurola, J., Knorr, W., Ladstaetter-Weißenmayer, A., Mota, B., Oom, D., Pacyna, J., Panasiuk, D., Pereira, J., Pulles, T., Pyle, J., Rast, S., Richter, A., Savage, N., Schnadt, C., Schulz, M., Spessa, A., Staehelin, J., Sundet, J., Szopa, S., Thonicke, K., van het Bolscher, M., van Noije, T., van Velthoven, P., Vik, A., and Wittrock, F.: REanalysis of the TROpospheric chemical composition over the past 40 years (RETRO) - A long-term global modeling study of tropospheric chemistry, Final Report, Tech. rep., Jülich/Hamburg, Germany, 2007.

Seinfeld, J. H. and Pandis, S. N.: Atmospheric Chemistry and Physics, John Wiley, New York, 1997.

Spiro, P. A., Jacob, D. J., and Logan, J. A.: Global inventory of sulfur emissions with 11 resolution, Journal of Geophysical Research: Atmospheres, 97, 6023–6036, doi:10.1029/91JD03139, URL http://dx.doi.org/10.1029/91JD03139, 1992.

Tegen, I., Harrison, S. P., Kohfeld, K., Prentice, I. C., Coe, M., and Heimann, M.: Impact of vegetation and preferential source areas on global dust aerosol: Results from a model study, Journal of Geophysical Research: Atmospheres, 107, AAC 14–1–AAC 14–27, doi:10.1029/2001JD000963, URL http://dx.doi.org/10.1029/2001JD000963, 4576, 2002.

von Kuhlmann, R.: Tropospheric Photochemistry of Ozone, its Precursors and the Hydroxyl Radical: A 3D-Modeling Study Considering Non-Methane Hydrocarbons, Ph.D. thesis, Johannes Gutenberg-Universität Mainz, Mainz, Germany, 2001.

von Kuhlmann, R., Lawrence, M. G., Crutzen, P. J., and Rasch, P. J.: A model for studies of tropospheric ozone and nonmethane hydrocarbons: Model evaluation of ozone-related species, Journal of Geophysical Research: Atmospheres, 108, doi:10.1029/2002JD003348, URL http://dx.doi.org/10.1029/2002JD003348, 4729, 2003.

Warwick, N. J., Pyle, J. A., Carver, G. D., Yang, X., Savage, N. H., O'Connor, F. M., and Cox, R. A.: Global modeling of biogenic bromocarbons, Journal of Geophysical Research: Atmospheres, 111, n/a–n/a, doi:10.1029/2006JD007264, URL http://dx.doi.org/10.1029/2006JD007264, d24305, 2006.